MULLARD LIMITED
Mullard House
Torrington Place
London, W.C.1

CONTENTS

Measurement of Desaturation Time-constant 66-72

Theoretical Analysis of Two-terminal Transistor Oscillator 73-77

Front Ends for 470Mc/s and 960Mc/s using the E88C 78-90

Tuned E.H.T. Transformer Converters 91-100

VOL. 7 No. 63 MARCH 1963

Mullard Technical Communications

VOLUME 7 NUMBER 63 **March 1963**

Mullard

Mullard Technical Communications

VOLUME 7 NUMBER 63 March 1963

Contents

Measurement of Desaturation Time-constant *D. F. Grollet and J. W. Thurston* 66

Theoretical Analysis of Two-terminal Transistor Oscillator *C. C. Hoo* 73

Front Ends for 470Mc/s and 960Mc/s using the E88C *A. R. Blake, J. Gregory, and J. C. Leguijt* 78

Tuned E.H.T. Transformer Converters *T. H. Beeforth* 91

Mullard Technical Communications contains information on the performance or application of Mullard products such as electronic valves and tubes, semiconductor devices and electrical and magnetic components. It is issued free-of-charge to equipment designers, research organisations, reference libraries and educational establishments. Bona fide applications to be added to the circulation list should be made under an official letter head to the Technical Information Department. Overseas enquiries should be addressed to the local Mullard agent, or to Mullard Overseas Ltd. at Mullard House.

Abstracts or references to an article should mention both the source, *Mullard Technical Communications*, and the authors. Requests for re-publication or translation should be made to the Editor in writing.

The issue of the information contained in this publication does not imply any authority or licence for the utilisation of any patented feature.

Mullard is the trade mark of Mullard Limited and is registered in most of the principal countries in the world.

This issue edited by

H. P. White (Editor-in-Chief) D. L. Evans F. A. Sowan E. G. Evans
M. O'Mahony

Published by

Technical Information Department
Mullard Limited, Mullard House, Torrington Place, London, W.C.1
LANgham 6633

© Mullard Limited, 1963

Made and Printed in England by
WIGHTMAN AND COMPANY LIMITED, 1/3 BRIXTON ROAD, LONDON, S.W.9

Measurement of Desaturation Time-constant

D. F. Grollet and J. W. Thurston
Mullard Semiconductor Measurement and Application Laboratory

The mathematical expression for the delay which occurs when a transistor is switched off from bottoming has two terms: one associated with the transistor itself, and the other with the circuit conditions. The inherent transistor component (the 'desaturation time-constant') has been directly measured by the charge extraction method. The values correlate adequately with values calculated from small-signal parameters, using the Ebers and Moll formula, and from measured values of desaturation time.

INTRODUCTION

When a transistor is operated in the bottomed region, with $I_{B(ON)} > I_C/h_{FE}$ (Fig. 1), there is a delay, after the instant of switch-off at the base, before the collector current begins to fall (Fig. 2). This delay t_s has been shown to be (Refs. 1, 2, 3)

$$t_s = \left[\frac{\dfrac{1}{\omega_{1N}} + \dfrac{1}{\omega_{1I}}}{1-\alpha_N\alpha_I}\right] \ln \frac{I_{B(ON)}+I_{B(OFF)}}{I_C/h_{FE}+I_{B(OFF)}} \qquad \ldots(1)$$

where $\omega_{1N} = 2\pi f_{1N}$ where f_{1N} is the normal cut-off frequency of the transistor, and $\omega_{1I} = 2\pi f_{1I}$ where f_{1I} is the inverse cut-off frequency. In all symbols, subscripts N and I denote normal and inverse operation.

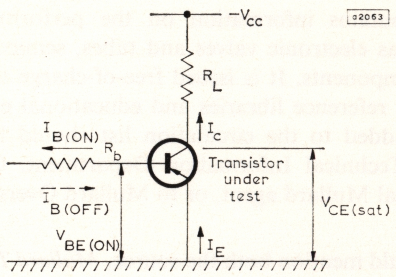

Fig. 1—Circuit configuration for bottomed transistor

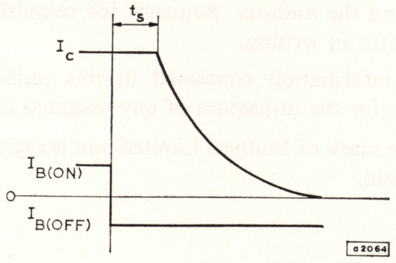

Fig. 2—Collector and base current waveforms at switch-off of bottomed transistor

The expression enclosed within square brackets involves transistor parameters only, and is thus a parameter itself and is called the desaturation time-constant τ_s.

Thus, by definition,

$$\tau_s = \frac{\dfrac{1}{\omega_{1N}} + \dfrac{1}{\omega_{1I}}}{1-\alpha_N\alpha_I}. \qquad \ldots(2)$$

The remaining terms in the expression for t_s describe the circuit conditions under which the transistor is used.

The desaturation time-constant τ_s may be indirectly determined by measuring the forward and inverse parameters of the transistor and calculating its value from Eq(2). This, however, is a laborious procedure. Alternatively, τ_s may be determined by measuring the delay t_s and calculating the value of τ_s for known values of $I_{B(ON)}$, $I_{B(OFF)}$, and I_C, using Eq(1). A third method, which will be described, allows the direct measurement of τ_s as the ratio of excess minority storage in the base region to excess base current.

BASIS OF METHOD OF MEASUREMENT

An account of the minority carrier concentration patterns and storage in the base region of a transistor when it is bottomed will be found in Ref. 4. Briefly, a transistor is said to be bottomed when the collector-base diode becomes forward biased. When this happens, there is a minority carrier concentration at the collector depletion layer boundary in the base region, in excess of the equilibrium level (Fig. 3). This means that a current flows from the collector region into the base; that is, in opposition to the normal collector current due to transistor action.

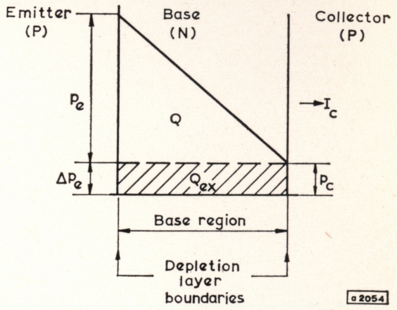

Fig. 3—Hole storage concentration in base region of bottomed transistor

In Fig. 3,

p_e = hole concentration in excess of equilibrium level, corresponding to a collector current I_C with a base current I_C/h_{FE}

$\Delta p_e = p_c$ = hole concentration in excess of equilibrium level, corresponding to an excess base current $I_{B(ON)}-I_C/h_{FE}$

Q_{ex} = charge due to excess base current

Q = charge corresponding to the current I_C.

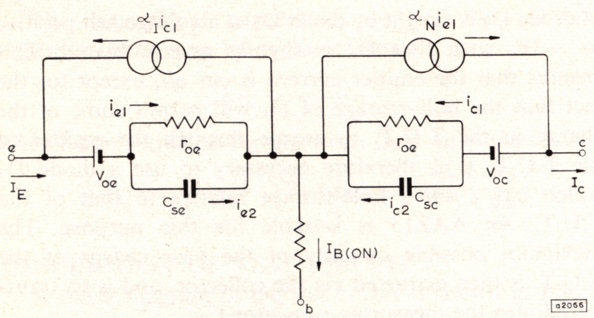

Fig. 4—Large-signal equivalent circuit for a bottomed transistor, showing currents flowing during switch-on Depletion-layer capacitances are omitted

In the equivalent circuit (Fig. 4) the opposing current is represented by i_{c1}, and the resultant steady-state current flowing in the collector circuit external to the transistor is

$$I_c = \alpha_N i_{e1} - i_{c1}. \qquad \ldots(3)$$

The steady-state base current is

$$I_{B(ON)} = i_{e1}(1-\alpha_N) + i_{c1}(1-\alpha_I), \qquad \ldots(4)$$

and the emitter current is the sum of the collector and base currents:

$$I_E = i_{e1} - \alpha_I i_{c1}. \qquad \ldots(5)$$

From Eqs(3) and (4) it can be shown that the base current in excess of that required to maintain the transistor just out of bottoming is

$$I_{B(ON)} - \frac{I_c}{h_{FE}} = \frac{i_{c1}}{\alpha_N}(1-\alpha_N\alpha_I). \qquad \ldots(6)$$

It has been shown (Ref. 1) that the charge in the base region of a bottomed transistor is

$$Q_b = \frac{i_{e1}}{\omega_{1N}} + \frac{i_{c1}}{\omega_{1I}}. \qquad \ldots(7)$$

Substituting for i_{e1} from Eq(3) and assuming $\alpha_N \simeq 1$, we find that

$$Q_b = \frac{I_c}{\omega_{1N}} + \frac{i_{c1}}{\alpha_N}\left(\frac{1}{\omega_{1N}} + \frac{1}{\omega_{1I}}\right).$$

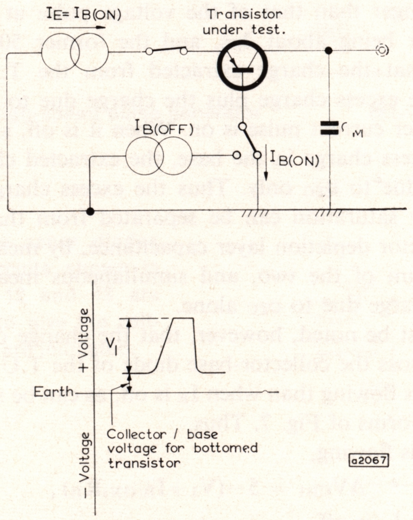

Fig. 5—Schematic of circuit for measurement of desaturation time-constant

Substituting for $\left(\dfrac{1}{\omega_{1N}} + \dfrac{1}{\omega_{1I}}\right)$ from Eq(2), we find that

$$Q_b = \frac{I_c}{\omega_{1N}} + \frac{i_{c1}}{\alpha_N}(1-\alpha_N\alpha_I)\tau_s.$$

And finally, from Eq(6),

$$Q_b = \frac{I_c}{\omega_{1N}} + \left(I_{B(ON)} - \frac{I_c}{h_{FE}}\right)\tau_s. \qquad \ldots(8)$$

(The charge on the collector depletion layer capacitance is neglected for the time being.)

Eq(8) reveals that the charge in the base region of a bottomed transistor is the sum of two parts, namely:

$\dfrac{I_c}{\omega_{1N}}$	+	$\left(I_{B(ON)} - \dfrac{I_c}{h_{FE}}\right)\tau_s$
Charge required to support a collector current I_c	+	Excess base charge, associated with the base current in excess of that required to maintain the transistor just out of bottoming.

For a transistor operating in the circuit configuration shown in Fig. 5, where the collector load consists of a capacitance C_M and the steady-state collector current I_c = zero, the charge built up in the base region is the excess charge associated with the excess base current $I_{B(ON)}$.

Thus

$$Q_b = I_{B(ON)}\tau_s. \qquad \ldots(9)$$

If the base and emitter of the transistor were to be suddenly open-circuited, this charge would be removed by an internal circulating recombination current having an initial value of $I_{B(ON)}$. If, however, a switch-off base current $I_{B(OFF)}$ is supplied to the transistor, and the emitter current is cut off, some of the charge is transferred through the collector circuit to the measuring capacitance C_M. It will be appreciated, therefore, that if the measured value of charge transferred to C_M is to approach the value of excess charge in the base, this charge must be transferred in a short time relative to the desaturation time-constant τ_s. To achieve this, $I_{B(OFF)}$ must be much larger than $I_{B(ON)}$, and its rise-time must be much shorter than τ_s.

The charge Q_b is then given by the product of the capacitance C_M and the peak voltage developed across it (V_1 in Fig. 5). Thus,

$$Q_b = V_1 C_M. \qquad \ldots(10)$$

(The charge removed from the collector depletion layer capacitance is, for the present, neglected.)

The desaturation time-constant is then

$$\tau_s = \frac{V_1 C_M}{I_{B(ON)}}. \qquad \ldots(11)$$

BASIC MEASURING CIRCUIT

The basic measuring circuit for τ_s is shown in Fig. 6. For the present discussion, the input to the emitter should be seen as a d.c. supply.

A constant current is passed through the emitter-base diode of the transistor under test (T.U.T.), through a resistance of 100Ω to earth. The collector is open-circuited to this d.c. current, since the collector load is a capacitance C_M to earth. Under these conditions the transistor is effectively bottomed, and the emitter current equals the base current $I_{B(ON)}$.

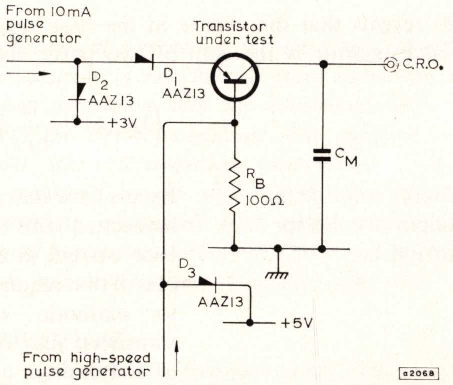
From 10mA pulse generator
Transistor under test
C.R.O.
D2 AAZ13
D1 AAZ13
+3V
RB 100Ω
CM
D3
AAZ13
+5V
From high-speed pulse generator
a2068

Fig. 6—Basic circuit for measurement of desaturation time-constant, including modified input to emitter

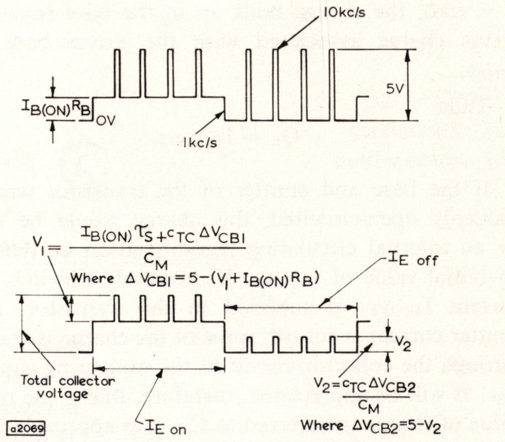
10kc/s
$I_{B(ON)}R_B$
0V
5V
1kc/s
$V_1 = \frac{I_{B(ON)}\tau_S + c_{TC}\Delta V_{CB1}}{C_M}$
Where $\Delta V_{CB1} = 5-(V_1+I_{B(ON)}R_B)$
I_E off
V_2
Total collector voltage
I_E on
$V_2 = \frac{c_{TC}\Delta V_{CB2}}{C_M}$
Where $\Delta V_{CB2} = 5 - V_2$
a2069

Fig. 7—Voltage waveforms at base (above) and collector (below) of transistor under test

A repetitive voltage pulse is applied to the base of the T.U.T. This pulse is obtained from a high-speed current-pulse generator (Fig. 10, page 69) capable of producing a voltage of 5V, with a rise-time of less than 2ns, across a resistive load of 100Ω. Since the T.U.T. represents a capacitive load across the 100Ω resistive load, the rise-time of voltage at the base will depend upon the type of T.U.T. Provided that this rise-time is short relative to the τ_s of the T.U.T. (say 1/10), reasonable accuracy of measured charge will be obtained.

When the base is thus driven positive, the emitter is cut off, the emitter current being diverted into an alternative path provided by diode D_2. The voltage at the anode of diode D_1 is caught by diode D_2 at a voltage just positive to +3V, such that D_1 is slightly reverse biased. This ensures that the emitter current is cut off, except for the fact that the hole-storage of D_1 will permit some of the charge in the T.U.T. to escape through the emitter of the T.U.T. It is therefore necessary to use a diode D_1 which has a small hole-storage relative to that of the T.U.T. An AAZ13 is suitable for this purpose. The maximum possible quantity of the base charge of the T.U.T. is then extracted via the collector, and is so transferred into the measuring capacitor C_M.

EFFECT OF COLLECTOR DEPLETION LAYER CAPACITANCE

The passage of current $I_{B(ON)}$ through the 100Ω resistor to earth will cause the base voltage to be positive to earth by $I_{B(ON)}R_B$. For a typical measuring current of 10mA this would be 1·0V. The emitter and collector diodes are both forward biased, so that at the collector the voltage will be $\simeq I_{B(ON)}R_B$. The base is then driven positive by a voltage of about 5V, so that the change of voltage across the collector depletion-layer capacitance is given by

$$\Delta V_{CB1} = 5 \cdot 0 - (V_1 + I_{B(ON)}R_B).$$

Since the voltage V_1 across the measuring capacitor is usually kept to a low amplitude (say 1·0V) the voltage swing across the large-signal collector depletion capacitance c_{TC} is of the order of 3V. The charge acquired by C_M includes the charge due to c_{TC}, and in some transistor types this may be large enough to warrant its measurement and subtraction from the total charge given by $(V_1 . C_M)$, in order to arrive at the correct value of excess charge.

In order to achieve this the basic measuring circuit is modified so that, instead of a constant d.c. current supply to the emitter of the T.U.T., a pulsed current is used. The modified circuit is that shown in Fig. 6, and the relevant waveforms are given in Fig. 7.

The pulse repetition rate at the emitter is about one-tenth that of the voltage pulse at the base; that is, about 1kc/s. The duration of the current pulse at the emitter is much longer than that of the voltage pulse at the base, the latter being about 2μs, and the former 500μs. This means that the charge extracted from the T.U.T. will equal the excess charge plus the charge due to c_{TC} when the emitter current pulse is on. When it is off, since there is no excess charge in the base, the extracted charge will be that due to c_{TC} only. Thus the excess charge due to transistor saturation can be separated from that due to the collector depletion layer capacitance, by measurement of the sum of the two, and simultaneous measurement of the charge due to c_{TC} alone.

It must be noted, however, that the change of voltage ΔV_{CB} across the collector-base diode of the T.U.T. is less when I_E is flowing than when I_E is off, as can be seen from the waveforms of Fig. 7. Thus,

when I_E is flowing,

$$\Delta V_{CB1} = 5 - (V_1 + I_{B(ON)}R_B),$$

and when I_E is off,

$$\Delta V_{CB2} = 5 - V_2.$$

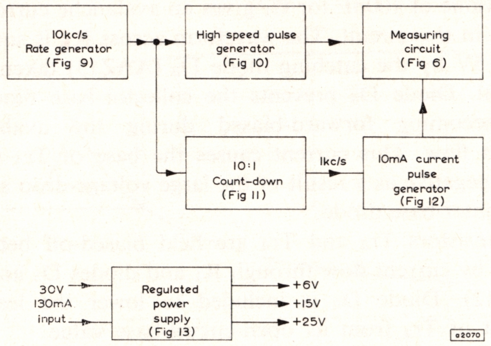
10kc/s Rate generator (Fig 9)
High speed pulse generator (Fig 10)
Measuring circuit (Fig 6)
10:1 Count-down (Fig 11)
1kc/s
10mA current pulse generator (Fig 12)
30V 130mA input
Regulated power supply (Fig 13)
+6V
+15V
+25V
a2070

Fig. 8—Block diagram of test-circuit

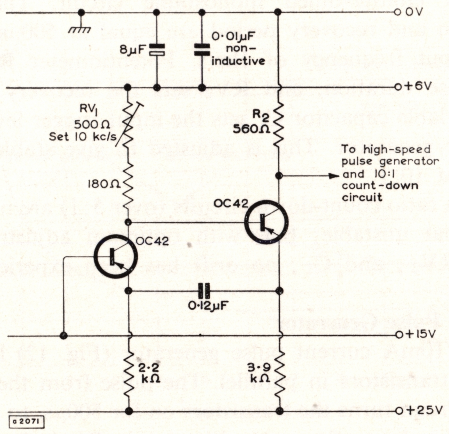
0V
8μF
0·01μF non-inductive
+6V
RV1 500Ω Set 10 kc/s
R2 560Ω
To high-speed pulse generator and 10:1 count-down circuit
180Ω
OC42
OC42
0·12μF
+15V
2·2 kΩ
3·9 kΩ
+25V
a2071

Fig. 9—Rate generator

The large-signal capacitance c_{TC} of the collector depletion layer may be evaluated from

$$c_{TC} = \frac{C_M . V_2}{5 - V_2}.$$

The charge extracted via c_{TC} when I_E is on is then

$$\Delta V_{CB1} . c_{TC} = [5 - (V_1 + I_{B(ON)}R_B)]\frac{C_M . V_2}{5 - V_2}.$$

DESCRIPTION OF TEST CIRCUIT

A block diagram of the test circuit is shown in Fig. 8. A rate generator, operating at 10kc/s, is used to trigger a high-speed pulse generator. This produces a 2μs 50mA fast-rise pulse which is applied to the measuring circuit. The rate generator output is also applied to a 10:1 count-down circuit. The 1kc/s output is used to drive a pulse generator which feeds 10mA pulses of 500μs duration to the measuring circuit.

The circuits of these units, and of a suitable power supply, are shown in Figs. 9 to 13. The measuring circuit has already been given (Fig. 6).

Rate Generator

The rate generator (Fig. 9) is an emitter-coupled multivibrator, using OC42 transistors. The potentiometer RV_1 is used to set the p.r.f. to 10kc/s. A 5V 50μs pulse is developed across R_2.

High-speed Pulse Generator

The high-speed pulse generator (Fig. 10) is made up of two circuits. The first is an emitter-coupled monostable, Tr_1 and Tr_2 (OC170 transistors), triggered by the output pulse of the rate generator at 10kc/s. The pulse duration produced is 2μs, amplitude 5V, rise and fall times 40ns. Two OA47 diodes, D_1 and D_2, are included in the emitter leads to prevent reverse bias breakdown of the emitter-base diodes.

This circuit is followed by an avalanche circuit Tr3 (an ASZ23 transistor) which is triggered by the 2μs pulse. Avalanche current flows from the Tr3 collector, through C_1 and R_B, and then via the 6V rail to the emitter-base diode of Tr_4 and the emitter of Tr_3. Thus a fast leading edge (2ns) is developed across R_B, and Tr_4 has a large turn-on charge fed to its base. At the end of the avalanche current pulse, Tr_4 will have been turned on to bottoming, and 50mA will flow through R_B for the remainder of the 2μs period.

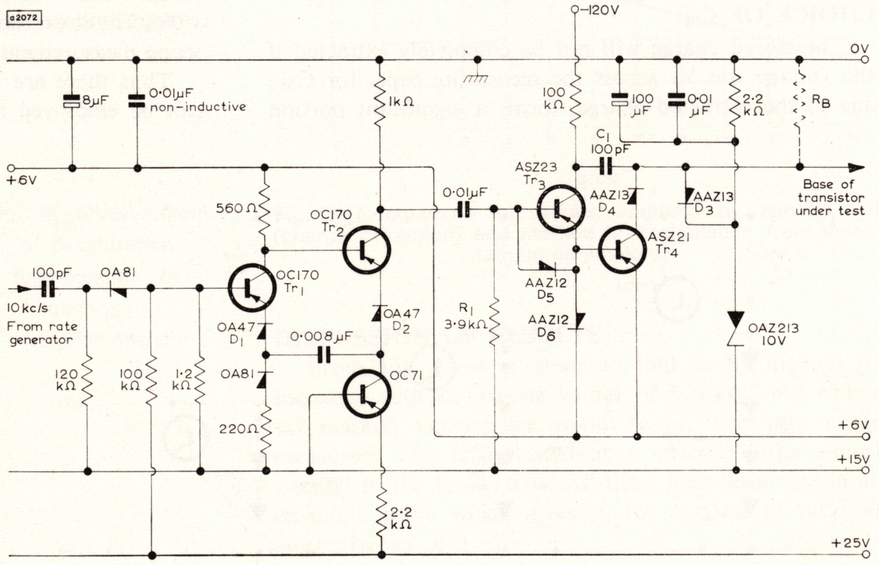
a2072
-120V
0V
8μF
0·01μF non-inductive
1kΩ
100 kΩ
100 μF
0·01 μF
2·2 kΩ
RB
C1 100pF
+6V
ASZ23 Tr3
AAZ13 D4
AAZ13 D3
Base of transistor under test
560Ω
OC170 Tr2
0·01μF
ASZ21 Tr4
100pF
OA81
OC170 Tr1
10kc/s From rate generator
AAZ12 D5
OA47 D2
OA47 D1
0·008μF
R1 3·9kΩ
AAZ12 D6
OAZ213 10V
OA81
OC71
120 kΩ
100 kΩ
1·2 kΩ
220Ω
+6V
+15V
2·2 kΩ
+25V

Fig. 10—High-speed pulse generator

Note: The zener diodes in the circuits shown in Figs. 10, 12 and 13 are selected to give the voltages that are indicated.

A value of 100pF for C_1 gives an avalanche current of 60mA in this circuit. The waveform across R_B is squared off at 5V by the catching diode D_3 (AAZ13) taken to a 5V rail. Diode D_4 prevents the collector-base diode of Tr_4 becoming forward-biased during the avalanche current flow. This current causes the base of Tr_4 to be taken negative as a result of the large voltage-drop across the emitter-base diode.

Transistors Tr_3 and Tr_4 are held biased-off between pulses by current flow through R_1 and diodes D_5 and D_6 (AAZ12). Diode D_6 is included to lower the leakage current of Tr_4 from its open-circuit-base value.

Count-down Circuit

The 10:1 count-down circuit (Fig. 11) is an emitter-coupled emitter-timed monostable circuit. The pulse duration and recovery period are equal at 500µs, giving an output frequency of 1kc/s. Potentiometer RV_1 sets the pulse duration, and RV_2 sets the recovery period. The variable capacitor C_1 sets the input trigger level from the rate generator. This is adjusted to give stable count-down at 10:1.

High ratio count-down circuits (over 5:1) are normally somewhat unstable; but, with optimum adjustment of RV_1, RV_2, and C_1, no drift has been experienced.

Current Pulse Generator

The 10mA current pulse generator (Fig. 12) has two OC170 transistors in parallel. The pulse from the count-down circuit turns the transistors on for 500µs, to provide a 10mA pulse to the measuring circuit. Diode D_1 is used to protect the emitter-base diodes of the OC170s under reverse-bias conditions. Potentiometer RV_2 sets the current pulse level to 10mA. The output can be changed from 1kc/s pulses to d.c. by the switch in the base circuit; and RV_1 sets the d.c. level to 10mA.

Power Supply

The power supply circuit is shown in Fig. 13. Three emitter-followers are used to provide stabilised voltage rails of +25V, +15V, and +6V, with respect to earth.

CHOICE OF C_M

The stored charge will not be completely extracted if the voltage rise V_1 across the measuring capacitor C_M, due to the extracted charge, forms a significant portion of the high-speed 5V pulse applied to the base of the transistor under test (Fig. 6). Measurements of τ_s and V_1, with various values of C_M, were carried out on an OC41 and an OC84. The results are plotted in Figs. 14 and 15. It is seen that the measured value of τ_s by this method falls sharply if V_1 is allowed to exceed about 1·0V. The lower limit of V_1 is 0·05V, as accurate oscilloscope measurements tend to be difficult below this value.

Thus there are limitations on the value of C_M which can be employed for a given transistor. A compromise must be made between the requirements given above for V_1. In practice, the following values of C_M have been found suitable for all transistors of the following types:

OC41, OC42, OC43: 30nF OC83, OC84: 100nF

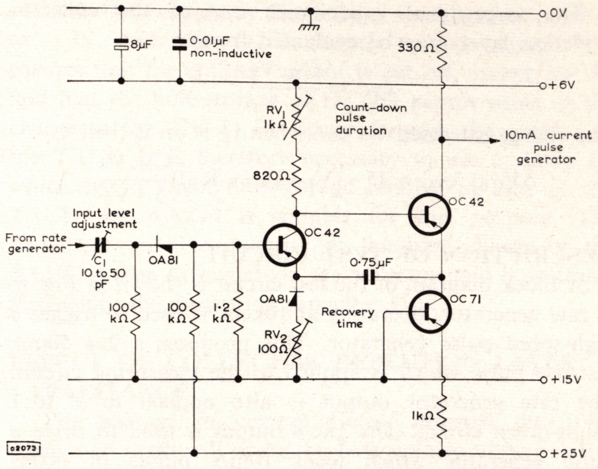
0V
8µF
0·01µF non-inductive
330Ω
+6V
RV1 1kΩ
Count-down pulse duration
10mA current pulse generator
820Ω
OC42
Input level adjustment
From rate generator
C1 10 to 50 pF
OA81
OC42
0·75µF
100 kΩ
100 kΩ
1·2 kΩ
OA81
Recovery time
OC71
RV2 100Ω
+15V
1kΩ
a2073
+25V

Fig. 11—Count-down circuit

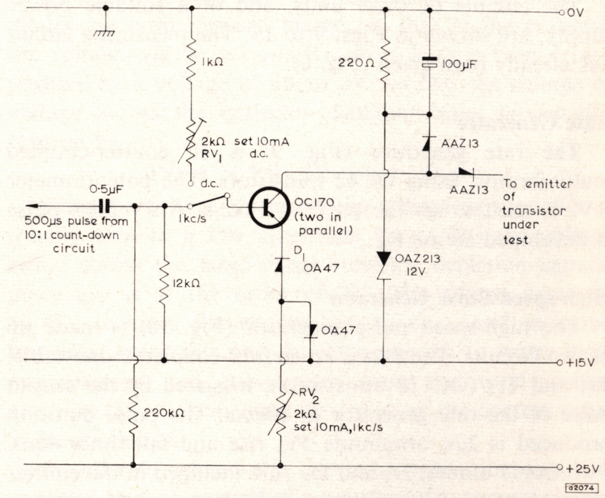
0V
1kΩ
220Ω
100µF
2kΩ RV1
set 10mA d.c.
AAZ13
d.c.
AAZ13
To emitter of transistor under test
0·5µF
500µs pulse from 10:1 count-down circuit
1kc/s
OC170 (two in parallel)
D1 OA47
OAZ213 12V
12kΩ
OA47
+15V
RV2 2kΩ set 10mA, 1kc/s
220kΩ
+25V
a2074

Fig. 12—Current pulse generator

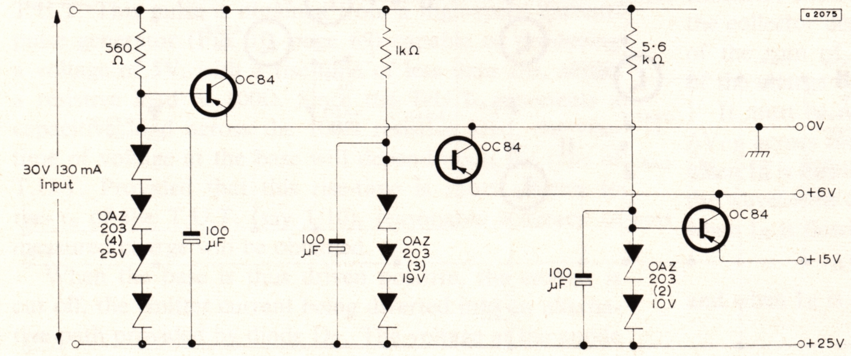
a2075
560 Ω
OC84
1kΩ
5·6 kΩ
0V
OC84
30V 130 mA input
OAZ 203 (4) 25V
100 µF
100 µF
OAZ 203 (3) 19V
+6V
OC84
+15V
100 µF
OAZ 203 (2) 10V
+25V

Fig. 13—Power supply

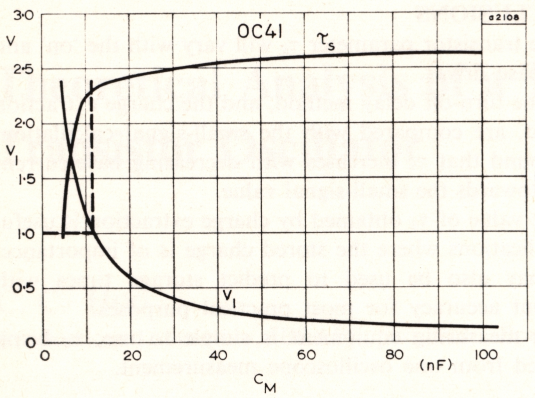

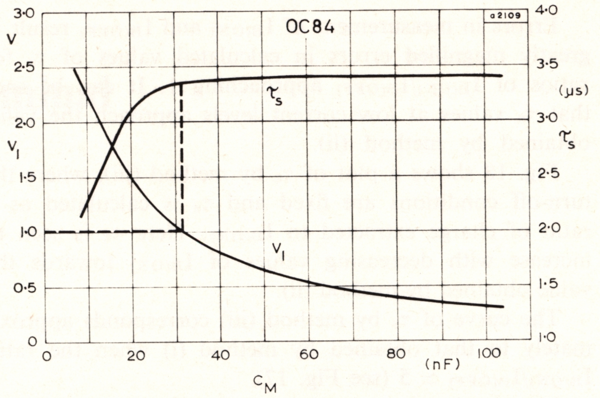

Figs. 14 and 15—Effect of variation of measuring capacitance on the measured value of desaturation time-constant
Results are shown for the OC41 and the OC84

COMPARISON OF CHARGE EXTRACTION WITH OTHER METHODS

The introduction gave three methods of measuring τ_s. These are:

(i) By calculating from t_s measurements taken in the circuit of Fig. 16, using Eq(1). Thus

$$\tau_s = \frac{t_s}{\ln \dfrac{I_{B(OFF)} + I_{B(ON)}}{I_C/h_{FE} + I_{B(OFF)}}}.$$

(ii) By calculation from measured forward and inverse small-signal parameters, using Eq(2). Thus

$$\tau_s = \frac{1/\omega_{1N} + 1/\omega_{1I}}{1 - \alpha_N \alpha_I}.$$

(iii) By the charge extraction method, using Eq(9). Thus

$$\tau_s = \frac{Q_B}{I_{B(ON)}}.$$

Measurements have been made by all three methods on a number of samples, and typical results are shown in Figs. 17 and 18 for an OC41. These graphs show variation of τ_s with the circuit parameters $I_{B(ON)}$ and $I_{B(OFF)}$ for these methods. The value of τ_s obtained by method (ii) is indicated by a straight line in both figures.

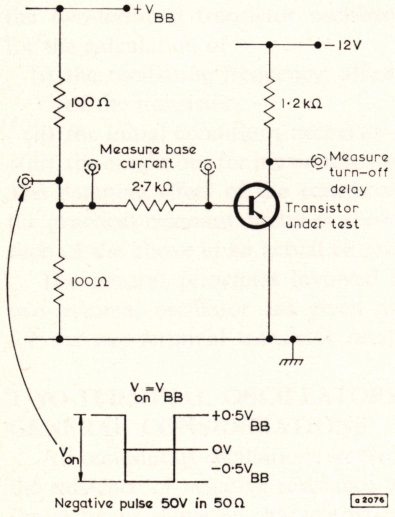
+VBB
−12V
100Ω
1·2kΩ
Measure base current
2·7kΩ
Measure turn-off delay
Transistor under test
100Ω
Von=VBB
+0·5VBB
0V
−0·5VBB
Von
Negative pulse 50V in 50Ω
a2076

Fig. 16—Measurement of desaturation time-constant by method (i) (turn-off delay)

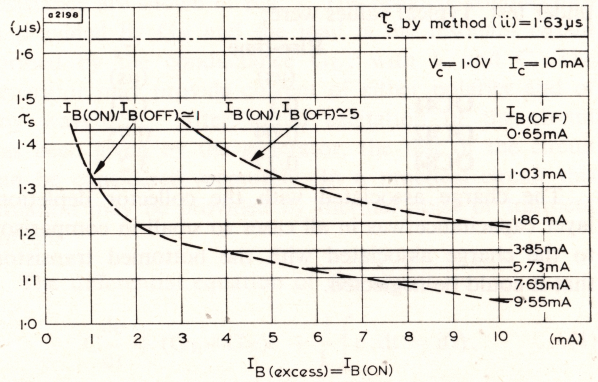

Fig. 17—Comparison of results obtained by method (i) (turn-off delay) and method (ii) (calculation from small-signal parameters)
The full lines represent the values obtained at various values of $I_{B(OFF)}$. The broken lines indicate ratios of $I_{B(ON)}$ to $I_{B(OFF)}$

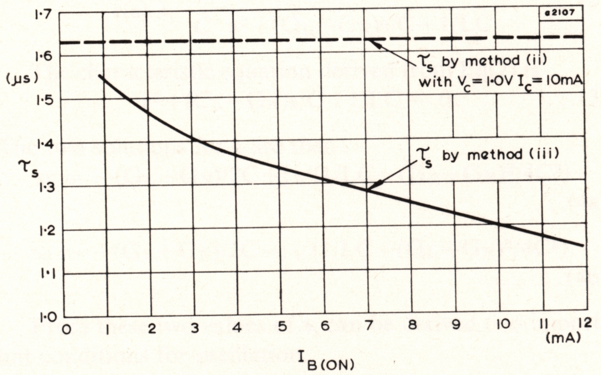

Fig. 18—Comparison of results obtained by method (iii) (charge extraction) and method (ii) (calculation from small-signal parameters)

DISCUSSION OF RESULTS

From Fig. 17 it is observed that τ_s by method (i) increases with decreasing values of $I_{B(OFF)}$, but shows no marked dependence upon $I_{B(ON)}$ over the range measured. This is indicated by a series of lines almost parallel to the $I_{B(ON)}$ axis. All these lines terminate in an envelope curve which gives τ_s for a constant ratio of $I_{B(ON)}/I_{B(OFF)} = 1$.

Errors in measurement of $I_{B(ON)}$ and $I_{B(OFF)}$ result in greatly magnified errors in calculated values of τ_s for ratios of $I_{B(ON)}/I_{B(OFF)}$ approaching 1. It can be seen that τ_s values at low current levels approach the value obtained by method (ii).

Fig. 18 shows a plot of τ_s by method (iii), where the turn-off conditions are fixed and τ_s is calculated as a ratio of charge extracted to $I_{B(ON)}$. Here τ_s is seen to increase with decreasing values of $I_{B(ON)}$ towards the value obtained by method (ii).

The curve of τ_s by method (iii) corresponds approximately to that obtained by method (i) when the ratio $I_{B(ON)}/I_{B(OFF)} \simeq 5$ (see Fig. 17).

It was pointed out on page 68 that the rise-time of the high-speed current pulse will be degraded when applied to the base of the transistor under test. Measured rise-times were all less than one-tenth of the τ_s of the transistor under test. Typical values were:

	Rise-time (μs)	τ_s (μs)
OC41	0·1	1·21
OC42	0·09	0·95
OC84	0·23	3·2

The charge associated with the collector depletion-layer capacitance was in all cases so small in comparison to the charge associated with the bottomed transistor, that it could be neglected.

CONCLUSIONS

The transistor parameter τ_s will vary with the 'on' and 'off' base drives.

If the turn-off delay method, and the charge extraction method, are compared with the small-signal calculation, it is found that τ_s increases with decreasing base-current levels towards the small-signal value.

The value of τ_s obtained by charge extraction is useful in applications where the stored charge is of importance, and may also be used to predict storage times with sufficient accuracy for most practical purposes.

The measuring equipment is simple to use, τ_s being obtained from one oscilloscope measurement.

REFERENCES

1. EBERS, J. J. and MOLL, J. L. 'Large-Signal Behaviour of Junction Transistors'. **Proc. I.R.E.,** Vol. 42, No. 12, Dec. 1954, pp. 1761 to 1772.
2. MOLL, J. L. 'Large-Signal Transient Response of Junction Transistors'. **Proc. I.R.E.,** Vol. 42, No. 12, Dec. 1954, pp. 1773 to 1784.
3. JAMES, P. and NEWELL, A. F. 'Switching Times for Alloy Junction Transistors'. **Mullard Technical Communications,** Vol. 5, No. 44, June 1960, pp. 159 to 171.
4. LE CAN, C. 'Transient Behaviour and Fundamental Transistor Parameters'. **Electronic Applications,** Vol. 20, No. 2, 1959/60, pp. 56 to 83.

Theoretical Analysis of a Two-terminal Transistor Oscillator

C. C. HOO
Applications Laboratory, IBRAPE, Sao Paulo, Brazil

The theory of a two-terminal transistor oscillator is considered, and this provides a method of evaluating the conditions necessary for oscillation to occur, the conditions for maximum amplitude of oscillation, the frequency, and the damping of the resonant circuit by the transistor.

INTRODUCTION

The two-terminal oscillator is the simplest form of oscillator circuit. It offers substantial advantages in circuits where switching of coils is used to obtain various frequency bands: the local oscillator in a multi-band superheterodyne wireless receiver is an example of such a circuit. The analysis, given in the following pages, of the two-terminal transistor oscillator provides formulae for the calculation of

(i) the oscillating frequency, allowing for the influence of the transistor,
(ii) the initial conditions necessary for oscillation,
(iii) the conditions for maximum amplitude of oscillation.

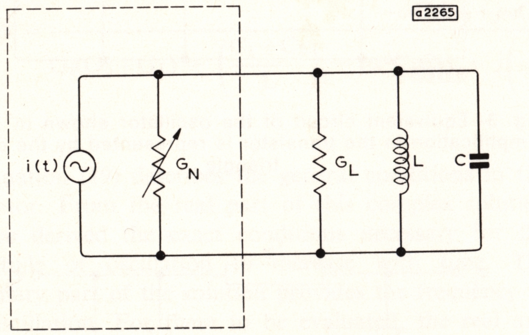

Fig. 1—The elements of a negative resistance oscillator

The damping effect of the transistor on the Q factor of the practical resonant circuit is allowed for in considering each of the above in an actual circuit.

The general principles involved in the action of any two-terminal oscillator are given and are then adapted for the two-terminal transistor oscillator.

TWO-TERMINAL OSCILLATORS: GENERAL CONSIDERATIONS

All continuous oscillations in electrical circuits require the existence of negative resistance which may be part of the static or dynamic characteristics of the device used. The elements of an oscillator circuit using negative resistance are shown in Fig. 1. The negative conductance is provided by G_N and the load is the resonant circuit formed by the conductance G_L, with L and C. The generator may provide current of either polarity and of any waveform. After initial excitation of the circuit has been given by the generator, the rest of the circuit can be considered separately. In a practical circuit this situation may be provided by thermal noise or transient current.

The differential equation of the circuit is:

$$C\frac{de}{dt} + (G_L+G_N)e + \frac{1}{L}\int e.dt = i(t). \qquad \ldots(1)$$

If we consider that at time t the current in the inductor, and the charge on the capacitor, are zero, the Laplace transform may conveniently be used. The solution to the equation then is

$$e(s) = \frac{i(s)}{C}\cdot\frac{1}{s^2+(G_L+G_N)s/C+1/LC}. \qquad \ldots(2)$$

The characteristic equation derived from Eq(2) is

$$s^2+(C_L+G_N)s/C+1/LC = 0. \qquad \ldots(3)$$

The two solutions for s are then

$$s_1 = -(G_L+G_N)/2C+j\sqrt{(1/LC-(G_L+G_N)^2/4C^2)} \qquad \ldots(4a)$$

$$s_2 = -(G_L+G_N)/2C-j\sqrt{(1/LC-(G_L+G_N)^2/4C^2)}. \qquad \ldots(4b)$$

From these two values of s, can be derived two important conditions for oscillation.

(i) The two solutions s_1 and s_2 are conjugate complex numbers. To obtain a periodic oscillation the following condition must be fulfilled.

$$1/LC > (G_L+G_N)^2/4C^2. \qquad \ldots(5)$$

(ii) The real part of the two solutions controls the amplitude of oscillation. If the real part is positive the amplitude increases with time. If it is negative, the amplitude decreases with time. When it takes the value zero, the amplitude remains constant. Since the initial amplitude is small the value of the real part must be positive to enable the oscillation to attain any usable proportions.

Thus,

$$G_L + G_N < 0. \qquad \ldots(6)$$

As the amplitude increases towards a certain value the negative conductance G_N must decrease to provide an oscillation of constant amplitude, giving the condition

$$G_L + G_N = 0. \qquad \ldots(7)$$

Should this condition be unobtainable then, in practice, the amplitude will be limited by the linearity of the device, so that, on average over one cycle, the condition of Eq(7) will be satisfied. In this case, distortion of the waveform is unavoidable.

These two sets of conditions for a two-terminal oscillator may be applied to the transistor oscillator, and used to find its working conditions.

TWO-TERMINAL TRANSISTOR OSCILLATOR

The circuit of a transistor oscillator is shown in Fig. 2. The base of the transistor is kept at a constant voltage by the potential divider R_1 and R_2, while the operating current is determined by the value of R_e. The capacitor C_b acts as a short-circuit to the a.c. signal from the base to earth. Since the circuit is in the common-base configuration, the y-parameters for common base are used in the calculations. Details of these y-parameters are given in Appendix 1.

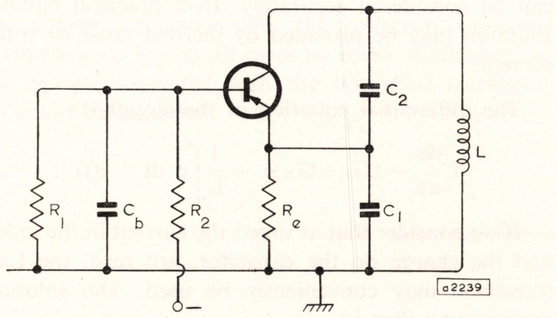

Fig. 2—Circuit diagram of transistor two-terminal oscillator

The action of the circuit is that of a common-base amplifier with a resonant circuit connected between the collector and earth, and with feedback occurring from the divider, C_1 and C_2, to the emitter. The feedback is positive because the emitter and collector, or input and output, have the same polarity in current changes in the common-base configuration.

The resonant circuit is formed by C_1, C_2 and L. The load conductance G_L is determined by the Q factor of the resonant circuit. At the resonant frequency the load admittance (Y_L) is given by the equation,

$$Y_L = G_L = \frac{1}{\omega LQ} = \frac{\omega C}{Q} \qquad \ldots(8)$$

where C is the capacitance of C_1 in series with C_2.

The output admittance (Y'_o) of an amplifier with feedback is given by the equation,

$$Y'_o = Y_o(1-\beta A_o) \qquad \ldots(9)$$

where Y_o is the open-loop output admittance of the amplifier, β is the voltage feedback ratio, and A_o is the open-loop voltage amplification. When βA_o is greater than unity the output admittance Y'_o is negative. Thus, with the condition for oscillation expressed in Eq(6), it is necessary that, for this feedback oscillator,

$$|Y'_o| > G_L. \qquad \ldots(10)$$

The above considerations apply to the circuit of Fig. 2, and a more extensive analysis of the conditions existing in this circuit is now given.

Equivalent Circuit of the Transistor Two-terminal Oscillator

The circuit of Fig. 3 shows the a.c. path through the oscillator circuit, shown in the equivalent-circuit form. The amplifier is taken as having an open-loop gain of A_v, an input conductance G_i and an output conductance G_o. The load consists of the conductance G_L and the resonant circuit formed by L, C_1 and C_2. The input and output susceptance of the amplifier are included in the equivalent load circuit.

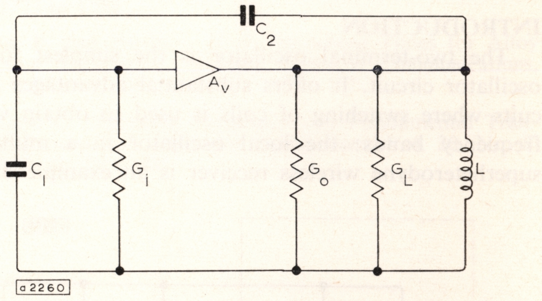

Fig. 3—Equivalent circuit of the oscillator shown in Fig. 2. Amplification in the transistor is represented by the central triangle

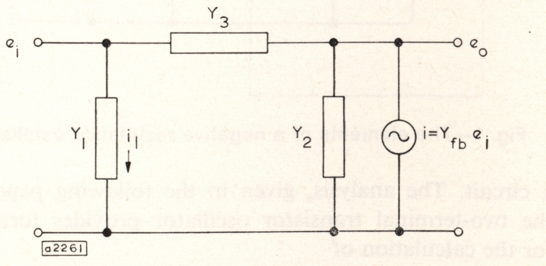

Fig. 4—Simplification of the oscillator equivalent circuit.

The circuit of Fig. 3 may then be more conveniently re-drawn as shown in Fig. 4. This consists of the three admittances, Y_1, Y_2 and Y_3 with the amplifier replaced by a current generator. The relationship between these two forms of equivalent circuit is contained in the three equations

$$Y_1 = G_i + j\omega C_1 \qquad \ldots(11)$$

$$Y_2 = G_o + G_L + \frac{1}{j\omega L} \qquad \ldots(12)$$

$$Y_3 = j\omega C_2. \qquad \ldots(13)$$

The voltage across Y_1 is denoted by e_i and that across Y_2 by e_o. The current through Y_1 is i_1 and the current through the generator is $y_{fb}e_i$. The terms i_1 and e_i may be described by the following equations.

$$i_1 = e_o\frac{Y_1Y_3}{Y_1+Y_3} \qquad \ldots(14)$$

$$e_i = \frac{i_1}{Y_1} = \frac{e_oY_3}{Y_1+Y_3}. \qquad \ldots(15)$$

The voltage feedback factor β is given by

$$\beta = \frac{e_i}{e_o} = \frac{Y_3}{Y_1+Y_3}. \qquad \ldots(16)$$

The voltage gain A_v may then be derived from Eq(34) in Appendix 1.

$$A_v = \frac{y_{fb}}{Y_2 + \dfrac{Y_1Y_3}{Y_1+Y_3}} = \frac{y_{fb}(Y_1+Y_3)}{Y_1Y_2+Y_2Y_3+Y_1Y_3} \qquad \ldots(17)$$

Oscillation can then occur when $A_v\beta$ equals unity, that is, when

$$A_v\beta = \frac{y_{fb}Y_3}{Y_1Y_2+Y_2Y_3+Y_1Y_3} = 1. \qquad \ldots(18)$$

Into this latter equation can be substituted the Eqs (11), (12) and (13) and also the substitution that $y_{fb} = g_{fb}+jb_{fb}$. This then gives the equation

$$A_v\beta = \frac{j\omega C_2(g_{fb}+jb_{fb})}{(G_i+j\omega C_1)\left(G_o+G_L+\dfrac{1}{j\omega L}\right)+\left(G_o+G_L+\dfrac{1}{j\omega L}\right)(j\omega C_2)+(G_i+j\omega C_1)(j\omega C_2)}$$

This then can be written

$$A_v\beta = \frac{-\omega C_2b_{fb}+j\omega C_2g_{fb}}{G_i(G_o+G_L)+\left(\dfrac{C_1+C_2}{L}\right)-(\omega^2C_1C_2)+j\left(\omega(C_1+C_2)(G_o+G_L)+\omega C_2G_i-\dfrac{G_i}{\omega L}\right)} \qquad \ldots(19)$$

Equation (19) describes the general conditions in the oscillator. From the real part of this complex solution can be derived the exact conditions necessary for the amplitude of oscillation to increase with time. The imaginary part of the solution provides the frequency of the oscillation. For these to be evaluated, the real and imaginary parts of Equation (19) must be separated. The critical condition for oscillation to occur is, however, that $A_v\beta$ equals unity, and this fact facilitates the separation of the two parts.

Frequency of Oscillation

The real part of Eq (19), with $A_v\beta = 1$, gives

$$G_i(G_o+G_L)+\frac{C_1+C_2}{L}-\omega^2C_1C_2+\omega C_2b_{fb} = 0.$$

Thus

$$\omega = \frac{-C_2b_{fb}\pm\sqrt{\left\{C_2^2b_{fb}^2+4C_1C_2\left(G_i(G_o+G_L)+\dfrac{C_1+C_2}{L}\right)\right\}}}{-2C_1C_2}$$

$$= \frac{b_{fb}}{2C_1}\pm\sqrt{\left(\frac{b_{fb}^2}{4C_1^2}+\frac{G_i(G_o+G_L)}{C_1C_2}+\frac{C_1+C_2}{C_1C_2L}\right)}.$$

The frequency may not take a negative sign, thus, assuming that $G_i(G_o+G_L)$ is positive, or if not, that $b_{fb}/2C_1$ is greater than the square root term,

$$\omega = \frac{b_{fb}}{2C_1}+\sqrt{\left(\frac{b_{fb}^2}{4C_1^2}+\frac{G_i(G_o+G_L)}{C_1C_2}+\frac{C_1+C_2}{C_1C_2L}\right)} \qquad \ldots(20)$$

The value of ω may be found by making simplifications which apply in some particular cases.

(i) In the idealised case it can be assumed that there is no phase shift in the transistor and that the effect, on loading, from the input conductance of the transistor, is negligible. The term b_{fb} is then equal to zero, and the term in G_i is negligible, so Eq(20) becomes

$$\omega = \sqrt{\left(\frac{C_1+C_2}{C_1C_2L}\right)}. \qquad \ldots(21)$$

This equation gives the value of ω at the natural frequency of the resonant circuit.

(ii) When the oscillator is working at a frequency well below its upper cut-off frequency, then only the term in b_{fb} may be neglected. Eq(20) then becomes

$$\omega = \sqrt{\left(\frac{C_1+C_2}{C_1C_2L}+\frac{G_i(G_o+G_L)}{C_1C_2}\right)}. \qquad \ldots(22)$$

Under these conditions the actual frequency of oscillation is slightly higher than the natural frequency determined by the L and C of the circuit.

(iii) When the oscillator works at a frequency approaching the upper cut-off frequency of the transistor, the value of b_{fb} is large and the term in G_i in Eq(20) becomes negligible in comparison and so Eq (20) becomes

$$\omega = \frac{b_{fb}}{2C_1}+\sqrt{\left(\frac{b_{fb}^2}{4C_1^2}+\frac{C_1+C_2}{C_1C_2L}\right)}.$$

If the term ω_o is then defined by the equation

$$\omega_o^2 = \frac{C_1+C_2}{C_1C_2L}$$

then the equation for ω becomes

$$\omega = \frac{b_{fb}}{2C_1}+\sqrt{\left\{\frac{b_{fb}^2}{4C_1^2}\left(1+\frac{4C_1^2\omega_o^2}{b_{fb}^2}\right)\right\}}.$$

The binomial expansion of this then gives

$$\omega \simeq \frac{b_{fb}}{C_1}+\frac{C_1\omega_o^2}{y_{fb}\sin\theta}+\cdots \qquad \ldots(23)$$

where θ is the phase angle of the transfer admittance.

Conditions Necessary for Oscillation

Putting the condition, that $A_v\beta$ equals unity, into Eq(19), and using only the imaginary parts, gives

$$(C_1+C_2)(G_o+G_L)+C_2G_i-C_2g_{fb}-\frac{G_i}{\omega^2L} = 0. \qquad \ldots(24)$$

The value of the ratio C_1/C_2 can be derived from this equation by eliminating the terms ω^2 and L. From Eq(21), in the ideal case

$$\omega^2 L = \frac{C_1+C_2}{C_1C_2}\,.$$

Replacing ω^2L in equation (24) then gives

$$(C_1+C_2)(G_o+G_L)+C_2(G_i-g_{fb}) - \frac{G_iC_1C_2}{C_1+C_2} = 0$$

that is

$$(C_1+C_2)^2(G_o+G_L)+C_2(C_1+C_2)(G_i-g_{fb})-G_iC_1C_2 = 0$$

that is

$$C_1^2(G_o+G_L)+2C_1C_2(G_o+G_L)+C_2^2(G_o+G_L)- \\ -C_1C_2g_{fb}+C_2^2G_i-C_2^2g_{fb} = 0$$

If this equation is then divided throughout by C_2^2 and rearranged, it becomes a quadratic equation in C_1/C_2 from which a solution, as follows, may be found.

$$\frac{C_1}{C_2} = \frac{-2(G_o+G_L)+g_{fb}+g_{fb}\sqrt{(1-4G_i(G_o+G_L)/g_{fb}^2)}}{2(G_o+G_L)}\,. \qquad \ldots(25)$$

When the oscillator frequency is below the cut-off frequency of the transistor, the term $4G_i(G_o+G_L)/g_{fb}^2$ is less than unity and so the binomial expansion then gives

$$\frac{C_1}{C_2} = -1 - \frac{G_i}{g_{fb}} + \frac{g_{fb}}{G_o+G_L}\,.$$

That is,

$$\frac{C_1}{C_2} = \frac{Y_{fb}\cos\theta}{G_o+G_L} - \left(1 + \frac{G_i}{Y_{fb}\cos\theta}\right) \qquad \ldots(26)$$

where θ is again the phase angle of the transfer admittance Y_{fb}. Eq(26) then gives the necessary ratio of C_1 to C_2 for oscillation to be possible.

Conditions for Maximum Oscillator Output

If the value of the negative conductance in the oscillator is plotted against the value of the ratio C_2/C_1 then the curve obtained is of the form indicated in Fig. 5. The maximum output of the oscillator is obtained with G_N at a maximum and this corresponds to a particular value of C_1/C_2. Operation at this maximum value of G_N also ensures oscillation with a wide range of transistor admittance. The value of the maximum can be obtained by differentiating the imaginary part of equation (19). This calculation is in Appendix 2 but the result is stated in Eq(27).

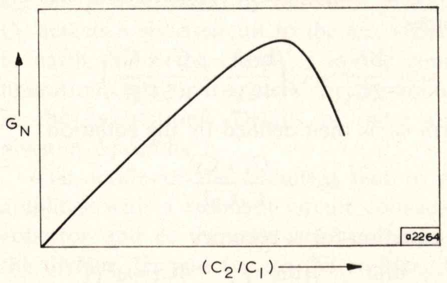

Fig. 5—G_n plotted against the ratio C_2/C_1

$$\frac{C_1}{C_2} = \sqrt{\left(\frac{G_i}{G_o+G_L}\right)}-1 \qquad \ldots(27)$$

The normal operating conditions in the oscillator will often be rather less favourable to maximum output than those indicated by this equation, especially as maximum output may be accompanied by poor frequency stability.

PRACTICAL DESIGN CONSIDERATIONS

A further useful factor k may be introduced, and the Eqs(26) and (27) may be expressed in terms of this factor in such a way as to facilitate circuit design. The value of the ratio of C_1/C_2 will normally lie between the values indicated by these two equations.

If the source admittance presented to the emitter of the transistor is Y_G, then it may be seen from Figs. 2 and 3 that at resonance, when Y_L is equal to G_L, the value of Y_G is given by

$$Y_G = \left(\frac{C_1+C_2}{C_2}\right)^2 (G_L+G_o)\,. \qquad \ldots(28)$$

As an approximation the term Y_L can be written as ky_{ob}, where k is a constant, and, similarly, Y_G can be written as ky_{ib}.
Then

$$\frac{Y_i}{Y_o} = \frac{(y_{ib}y_{ob}-y_{rb}y_{fb}+ky_{ib}y_{ob})(y_{ib}+ky_{ib})}{(y_{ib}y_{ob}-y_{rb}y_{fb}+ky_{ib}y_{ob})(y_{ob}+ky_{ob})}$$

or

$$\frac{Y_i}{Y_o} = \frac{y_{ib}}{y_{ob}}\,.$$

As previously mentioned, the susceptive part of the input and output admittance are included in that of the resonant circuit. Thus,

$$\frac{Y_i}{Y_o} = \frac{y_{ib}}{y_{ob}} = \frac{g_{ib}}{g_{ob}}\,. \qquad \ldots(29)$$

The factor k is not merely a mathematical device but an important design factor, and is an indication of the loading on the resonant circuit by the transistor. When this form of transistor two-terminal oscillator is being designed the value of k needs to be determined almost at the outset. The value of k equal to unity corresponds to the condition for maximum output, that is, impedance matching.

The value of the ratio C_1/C_2 in terms of k may be derived by substituting Eq(29) into Eq(26) and Eq(27). Substitution in Eq(26) gives the condition for self-starting oscillation to occur:

$$\frac{C_1}{C_2} = \frac{g_{ib}/k}{g_{ob}+G_L/k} - \left(1+\frac{g_{ib}}{g_{fb}(g_{ob}+G_L/k)}\right)$$

that is

$$\frac{C_1}{C_2} = \frac{(y_{fb}\cos\theta)/k}{g_{ob}+G_L/k} - \left(1+\frac{g_{ib}}{(y_{fb}\cos\theta)(g_{ob}+G_L/k)}\right)\,. \qquad \ldots(30)$$

Similarly, substitution in Eq(27) gives the condition for maximum output.

$$\frac{C_1}{C_2} = \sqrt{\left(\frac{kg_{ib}}{kg_{ob}+G_L}\right)}-1 = \sqrt{\left(\frac{g_{ib}}{g_{ob}+G_L/k}\right)}-1\,. \qquad \ldots(31)$$

The usual design-value of C_1/C_2 will lie between these two values, and be a compromise to give optimum output and stability of frequency.

APPENDIX 1

Transistor y-Parameters used in this article

Input Admittance (y_{in})

$$y_{in} = y_i - \frac{y_fy_r}{Y_L+y_o} \qquad \ldots(32)$$

Output Admittance (y_{out})

$$y_{out} = y_o - \frac{y_fy_r}{y_i+y_s} \qquad \ldots(33)$$

Forward Voltage Gain (V_2/V_1)

$$\frac{V_2}{V_1} = \frac{-y_f}{y_L+y_o} \qquad \ldots(34)$$

These parameters are related to the definitions given below:

y_{ib} = input admittance (output short-circuited)
y_{ob} = output admittance (input short-circuited)
y_{fb} = forward transfer admittance (output short-circuited)
y_{rb} = reverse transfer admittance (input short-circuited)

All of these refer to common-base configuration.

APPENDIX 2

Derivation of Value of C_1/C_2 for Maximum Output

The imaginary part of Eq(21) can be written:

$$A_v\beta = \frac{C_2g_{fb}}{(C_1+C_2)(G_o+G_L)+C_2C_i - \dfrac{G_i}{\omega^2L}}\,.$$

Then, substituting $\omega^2L = (C_1+C_2)/C_1C_2$ into this equation gives

$$A_v\beta = \frac{C_2g_{fb}}{(C_1+C_2)(G_o+G_L)+C_2G_i-G_iC_1C_2/(C_1+C_2)}$$

$$= \frac{C_2(C_1+C_2)g_{fb}}{(C_1+C_2)^2(G_o+G_L)+C_2(C_1+C_2)G_i-G_iC_1C_2}$$

$$= \frac{(C_1C_2+C_2^2)g_{fb}}{(C_1^2+2C_1C_2+C_2^2)(G_o+G_L)+C_2^2G_i}$$

$$= \frac{(C_1/C_2+1)g_{fb}}{[(C_1/C_2)^2+2C_1/C_2+1](G_o+G_L)+G_i}$$

$$= \frac{(a+1)g_{fb}}{(a^2+2a+1)(G_o+G_L)+G_i}$$

where $a = C_1/C_2$. Then, when differentiated with respect to a, this equation becomes:

$$\frac{d(A_v\beta)}{da} = \\ = \frac{g_{fb}[(a^2+2a+1)(G_o+G_L)+G_i]-(2a+2)(a+1)g_{fb}(G_o+G_L)}{[(a^2+2a+1)(G_o+G_L)+G_i]^2}$$

At a maximum value of the function, $d(A_v\beta)/da$ is zero. Hence,

$$g_{fb}[(a^2+2a+1)(G_o+G_L)+G_i] = (2a+2)(a+1)g_{fb}(G_o+G_L)$$

that is

$$G_i = (G_o+G_L)(a^2+2a+1)$$

that is

$$a = \frac{C_1}{C_2} = \sqrt{\left(\frac{G_i}{G_o+G_L}\right)}-1\,. \qquad \ldots(35)$$

Eq(35) has been already quoted as Eq(27).

Front Ends for 470Mc/s and 960Mc/s using the E88C

A. R. BLAKE J. GREGORY J. C. LEGUIJT
Mullard Applications Research Laboratory

The article describes the valve technology of the E88C u.h.f. triode and the performance at frequencies up to 1100Mc/s. Also described are single-stage amplifiers and receiver front ends for the 470Mc/s and 960Mc/s bands.

INTRODUCTION

The design specification for this valve was derived from the necessary u.h.f. performance in equipment working at frequencies up to 1000Mc/s. Receiver front-ends using the valve would need satisfactory r.f. amplifiers and local oscillator stages with good shielding between them, and a good overall noise factor. Each stage would thus need adequate power gain at frequencies up to 1000Mc/s, good stability, low feedback and low noise factor. The valve would also need to be free from local electrical resonances, especially for use in wideband applications.

The fulfilment of these requirements with a valve of conventional electrode structure is almost impossible if acceptable prices are to be maintained. Special valve structures can be built but many are again too expensive. The Mullard E88C has a design using components which are near to being conventional and are easily produced, and only the lay-out of components is unconventional. The desired performance is thus obtained in a valve which is not costly to produce.

This article describes the valve technology and performance of the E88C which is a special quality version of the EC88. The EC88 can be used in any of the applications given for the E88C but the same life and reliability performance may not be obtained. The E88C is designed to give long life as well as the electrical performance described.

Although this article is confined to examples of narrowband applications the E88C can be used in many wideband applications. Such wideband applications would include aerial amplifiers and converters used in signal distribution for u.h.f. television.

VALVE TECHNOLOGY

A consideration of the various features which influence the performance of a valve leads to the conclusion that some compromise is essential if excessive manufacturing costs are to be avoided. Many of the requirements of a u.h.f. valve are common, however, to all aspects of its performance.

Both high power gain and low noise factor are obtainable by ensuring a high value of mutual conductance and a low value of transit time. Power gain is also improved by a low output capacitance.

The main passive sources of feedback in a triode grounded-grid amplifier circuit are shown in Fig. 1a. They are the anode-to-cathode capacitance (c_{a-k}) and the grid lead inductance (L_g), the latter forming a common impedance to the currents circulating through the grid-to-cathode capacitance (c_{g-k}) and the anode-to-grid capacitance (c_{a-g}). The mutual inductance between the input and output connections is sufficiently small to be ignored. The impedances shown in Fig. 1a can be redrawn, by using the star-delta transform, in the form shown in Figs. 1b and 1c. The value of c_1 in Fig. 1c is given by the equation

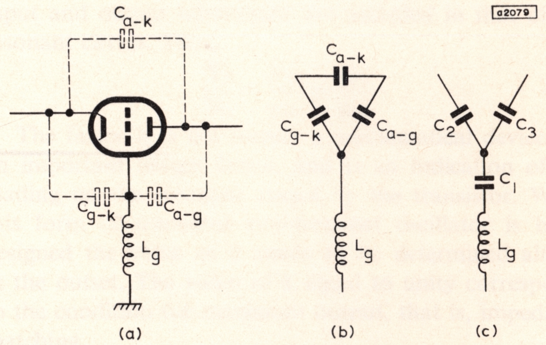

Fig. 1—Passive feedback paths in a grounded-grid triode
(a) internal sources of feedback
(b) equivalent circuit
(c) transformed equivalent circuit

$$c_1 = c_{g-k}+c_{a-g}+\frac{c_{g-k}.c_{a-g}}{c_{a-k}}.$$

The values of c_1 and L_g in Fig. 1c determine the self-neutralising frequency: self-neutralising occurs when the frequency of operation is the resonant frequency of c_1 and L_g. A high resonant frequency is obtained when c_{a-k} is large and both c_{g-k} and c_{a-g} are small, but large values of c_{a-k} cannot be tolerated because of the consequent increase in feedback. Good performance at u.h.f. therefore requires a compromise between the high value of self-neutralising frequency and a low value of c_{a-k}. Feedback is minimised by low values of c_{a-k}, c_{g-k}, c_{a-g} and L_g, and also by screening between cathode, heater and anode.

Low noise factor and high power gain are obtainable by ensuring high mutual conductance and small transit times but unfortunately these conditions imply close electrode spacing which causes high inter-electrode capacitances. Several compromises could be made, such as combining wider electrode spacing with high operating voltage to reduce transit time. Such a valve would be large and a more suitable compromise is obtained with reduced electrode areas and small clearances.

A suitable arrangement has been produced for the E88C electrodes. The performance of the valve meets the design specification, but although an unconventional electrode arrangement was essential, the cost has been kept to a level consistent with normal valves.

Electrode Structure

The various electrical characteristics of the E88C were to be obtained with a valve with a small electrode system. Investigation showed that the most suitable structure was an asymmetrical one, usually called single-sided, in which the anode was completely to one side of the cathode. One disadvantage of this single-sided structure is that there can be no compensation for spacing tolerances which affect performance, as there can be in a symmetrical structure. In particular, the grid-to-cathode spacing becomes very critical, whereas in the symmetrical structure the effects of small spacing on one side are largely offset by the increased spacing on the other. The problem is aggravated by the need for small grid-to-cathode clearance. The electrical advantages of the single-sided system, however, are so great, that to overcome the difficulties of construction is worthwhile.

A plan view of some of the components in position in the valve is given in Fig. 2. The three electrodes are shown with their connections to the valve-base pins. Each of the electrodes and other main features of the valve are described briefly below.

Anode

The shape of the anode is similar to the anodes used in many frame-grid valves. Capacitance between anode and cathode has been kept low by shaping the elongated 'nose' of the anode so that only a small working area is close to the cathode. The length of this nose is greater than any previously used in an anode of this type. The total area of the anode is large enough to permit the required dissipation. The length of the anode also permits anode connections to be made where they have only a small capacitance with the grid backbones.

Cathode

One side only of the cathode is used in the E88C, and so only this side is coated with the emissive paste. The paste coating is unusually thin and its dimensions are controlled with great accuracy. This is because slight variations in the thickness of the coating severely alter the characteristics of the valve where the gap between cathode and grid is small. The area of cathode is also a carefully chosen compromise: low area assists in minimising inter-electrode capacitances but also makes the current density unacceptably high. The arrangement in the E88C provides a satisfactory compromise between values of mutual conductance, grid-to-cathode clearance and cathode current density.

Grid

The grid of the E88C is symmetrical and is a normal frame grid wound on thick backbone wires. The frame grid is off-set about the cathode so that the active face of the cathode is close to one side of the grid wires with the anode just beyond this. The second side of the grid surrounds the rest of the cathode but is not close to it and is not in the stream of electrons from cathode to anode. The large backbones in the grid ensure that the unused side of the grid adds very little to the capacitances between the grid and the other electrodes.

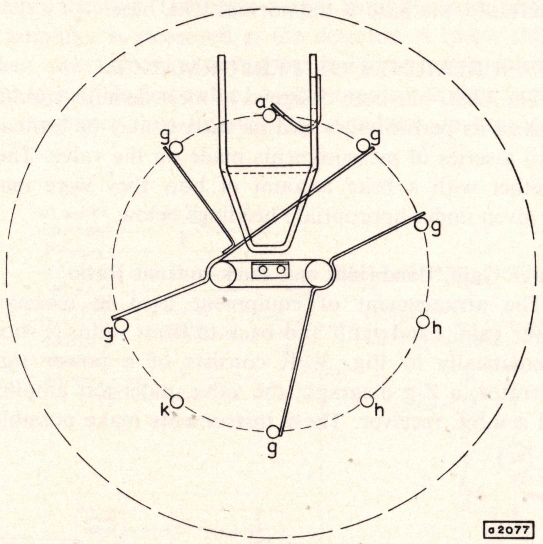

Fig. 2—Plan view of the electrode structure of the E88C

Because the frame grid is used in this asymmetrical way, the electrical properties of the single sided system are conserved. The frame grid itself, however, can be made by the conventional factory equipment and so the production costs of the valve can be kept low.

Connections between the grid backbones and the base pins are made with strips of metal which are silver-plated. Five connections are made to five separate pins and if all are used the grid-lead inductance is minimised. The five strips of metal are placed in the valve in such a way that they screen the anode from the cathode and heater: the valve will normally be in grounded-grid operation so that the anode-to-cathode capacitance is minimised.

Mica Supports and Glass Bulb

To increase the control over the small grid-cathode spacing the mica supports used with the E88C are of a special design. Tolerances on the micas have been considerably reduced from the usual values and the shape used is one designed to give maximum obtainable rigidity to the electrodes.

The bulb used is slightly tapered internally so that when the electrode assembly is put into the bulb a progressive tightening is applied to the micas. This again increases rigidity and assists in maintaining tolerances at the necessary values. (The EC88 uses a more normal form of mica and bulb.)

Glass Base

The base of the valve is a version of the B9A base, improved in a way to decrease the inductance of the leads. The glass cones surrounding each pin inside the valve have been decreased in height so that the electrode assembly can be mounted closer to the base with shorter leads. Externally, the base is the normal B9A base.

MEASUREMENTS OF PERFORMANCE

The E88C has been designed to meet definite specifications in its performance and its success may be estimated from a series of measurements made on the valve. These, together with a brief account of how they were made, are given under appropriate headings below.

Power Gain, Bandwidth and Back-to-front Ratio

The arrangement of equipment used in measuring power gain, bandwidth and back-to-front ratio, is shown schematically in Fig. 3. It consists of a power signal generator, a Z-g diagraph, the valve-under-test amplifier, and a u.h.f. receiver. These instruments make possible a simple and convenient measuring procedure which gives extremely repeatable and reliable measurements at the frequencies concerned.

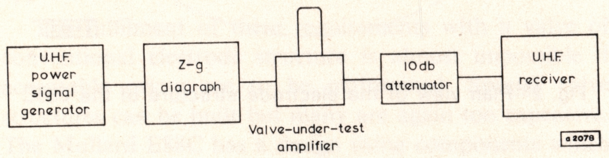

Fig. 3—Equipment used for measuring power gain, bandwidth, and back-to-front ratio

The diagraph provides a direct visual indication of either the input or the output impedance of the valve-under-test amplifier. Power gain is measured by the substitution method, using the attenuator in the receiver. This precision attenuator provides a range of 70dB in steps of 10dB, 1dB and 0·1dB. Bandwidth is measured by reducing the attenuator setting in the receiver by 3dB, and then varying together the signal generator frequency at constant output and receiver frequency either side of the original frequency until the indicated output of the receiver returns to its first value. The back-to-front ratio is the attenuation of signal passed from the output of the amplifier to the input and is measured by a substitution method with the signal connections reversed.

The circuit of the valve-under-test amplifier is given in Fig. 4. To match the generator output impedance to the valve input impedance for maximum power transfer, a π filter is used. The output circuit of the amplifier consists of a $\lambda/2$ trough-line tuned by a variable capacitor at the end of the line further from the valve. The bandwidth of the anode circuit is adjusted by varying the coupling between the load and the line. To prevent damping of the input circuit, r.f. chokes are used in series with the cathode bias resistor and in both of the heater leads. If a well-soldered screen is used between the input and output circuits then the E88C amplifier is stable, even with narrow bandwidth, at frequencies in excess of 1000Mc/s. The power gain, bandwidth and back-to-front ratio, measured at frequencies from 400Mc/s to 1100Mc/s with $\lambda/2$ and $\lambda/4$ trough-lines, are shown in Figs. 5 to 9.

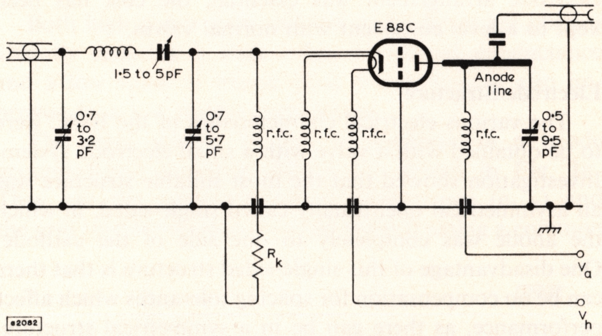

Fig. 4—Valve-under-test amplifier

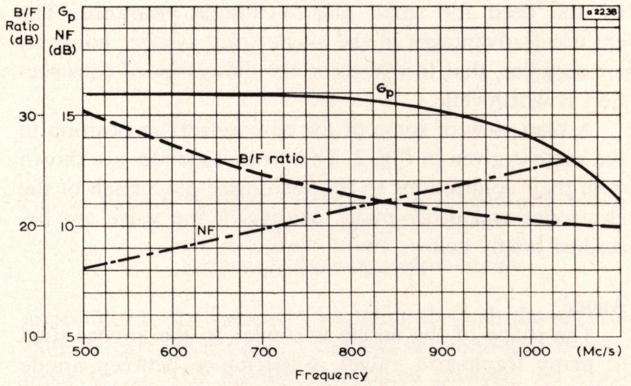

Fig. 5—Noise factor, power gain and back-to-front ratio of the E88C plotted against frequency, with a bandwidth of 12Mc/s

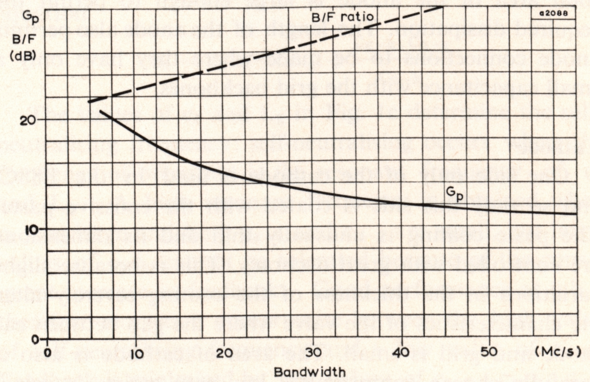

Fig. 6—Power gain and back-to-front ratio of the E88C at 1000Mc/s plotted against bandwidth, using a $\lambda/2$ line

Noise Factor

The measurements on noise factor for the E88C have been made with equipment specially developed in the Applications Research Laboratory for this purpose*. This was necessary since reliable and repeatable measurements of noise factor at frequencies approaching 1000Mc/s are difficult to obtain when using the commercial equipment generally available.

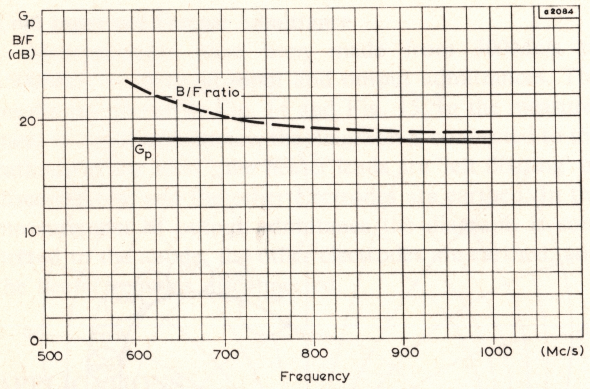

Fig. 7—Power gain and back-to-front ratio of the E88C plotted against frequency with a bandwidth of 12Mc/s and using a $\lambda/4$ line

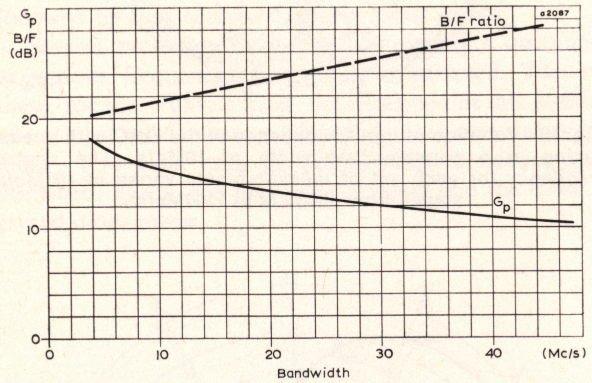

Fig. 8—Power gain and back-to-front ratio of the E88C at 600Mc/s plotted against bandwidth, using a $\lambda/4$ line

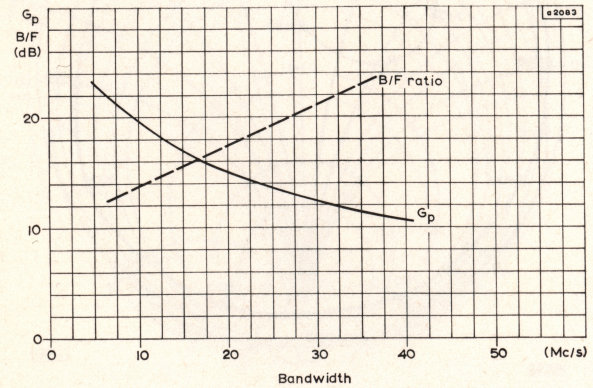

Fig. 9—Power gain and back-to-front ratio of the E88C at 1000Mc/s plotted against bandwidth, using a $\lambda/4$ line

The noise measurement equipment consists of a noise generator, valve-under-test amplifier, frequency converter with crystal-controlled local oscillator, intermediate frequency amplifier, and a detector with measuring instruments. The repeatability of this measuring equipment is improved by the use of stabilised heater supplies, pre-aged valves with gold-plated pins, gold-plated valve holder contacts, minimum numbers of plugs and sockets, relay switching where possible, and the crystal control of local oscillators.

The noise measurements are made with the equipment arranged as in Fig. 10. The noise generator is connected to the valve-under-test amplifier but is switched off and therefore inactive. The noise output from the valve-under-test amplifier is measured at the detector. A meter shunt is then switched in to bring the indicated noise reading down to half its first value. A measurement is then made, with the meter thus shunted, by switching on the noise source and raising its output until the noise level reading on the shunted meter is increased to the value it had previously. The noise level of the generator on this second reading is then the same as that from the valve-under-test amplifier in the first reading. The noise source used is a Rohde and Schwarz 'noise head' built into a separate chassis, and reliable repeatable noise measurements can be made at frequencies up to 1000Mc/s. The frequency converters enable noise factor measurements to be made at frequencies from 300Mc/s to 1000Mc/s in steps of 100Mc/s.

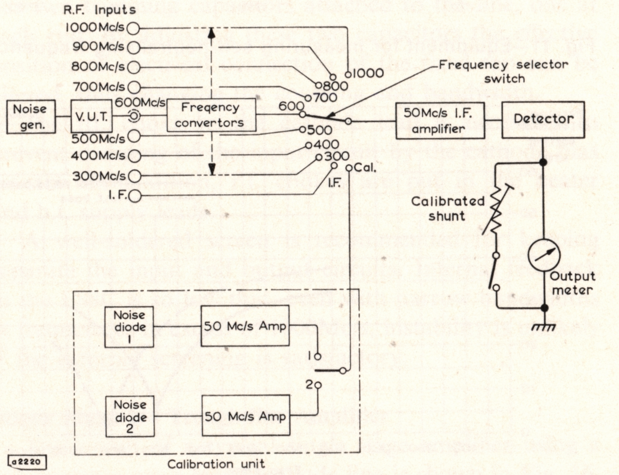

Fig. 10—Noise-measuring equipment

The method of noise measurement described measures the overall noise factor of the system of amplifiers. At low frequencies no correction is necessary because the gain of the valve-under-test can be made large and the noise factors of the other stages can be made low. At u.h.f., however, this is difficult and a correction for the residual noise of the rest of the equipment is usually necessary.

---

*The method is based on information taken from a Ministry of Aviation unpublished report 'An Equipment for Measuring Noise Factor at 45Mc/s', R. B. Wilson, March 1956.

The expression for the overall noise factor (N_o) of a system of amplifiers is:

$$N_o = N_1 + \frac{N_2-1}{G_1} + \frac{N_3-1}{G_1G_2} + \ldots\ldots$$

where N_1, N_2, . . . are the noise factors of the first, second and other stages, and G_1, G_2, . . . are the power gains of the same stages. In measuring the noise factor of the valve-under-test it is therefore essential to know the overall noise factor, the gain of the valve-under-test and the residual noise factor of the rest of the equipment. The residual noise factor can be found by making a measurement with the valve-under-test amplifier omitted.

In addition to the above correction a further correction must be applied to allow for the image response in the receiver. The correction is made by multiplying the measured noise factor by the term $(G_S+G_I)/G_S$ where G_S is the signal frequency gain and G_I is the image frequency gain.

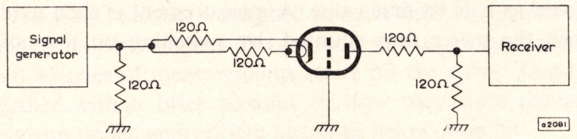

Fig. 11—Equipment for measuring self-neutralising frequency

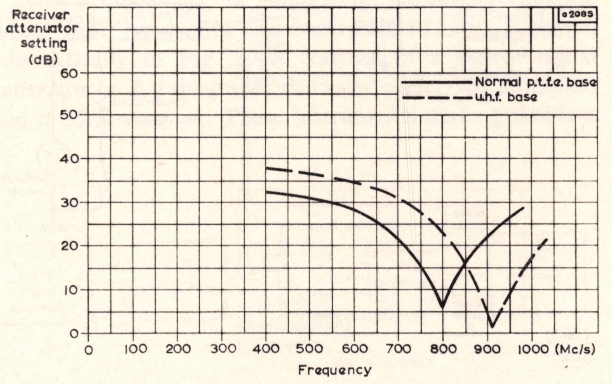

Fig. 12—Self-neutralising curve for the E88C

The noise factor measurements were made under conditions of power-matching in the input circuits of the valve-under-test: this was to obtain maximum repeatability.

The curve shown in Fig. 5 shows the variation of noise factor of the E88C with frequency, with the input circuit tuned for maximum power gain and with a λ/2 line at the output.

The noise factor of the E88C has been measured at various times in valves on life-test. The noise factor increases only slowly during extended periods of continuous operation of the valve. This represents an improvement on many u.h.f. valve types which have acceptable noise factors at the start of life but become noisy within short periods.

Feedback

To ascertain the extent of feedback in the E88C various measurements were made. They include measurement of back-to-front ratio, self-neutralising frequency and variation of input impedance with anode tuning. The back-to-front ratio has been mentioned previously under that heading.

The self-neutralising frequency is measured with the valve connected as shown in the circuit of Fig. 11. The valve and circuit are heavily screened. Applied to the input is a signal of variable frequency, but of constant amplitude. The receiver attenuator is set at each frequency to maintain the indicated output at a constant value. The curves of Fig. 12 show the attenuator setting versus the frequency: the self-neutralising frequency is affected by the type of valve holder employed, mainly because of the different value of grid lead inductance obtained.

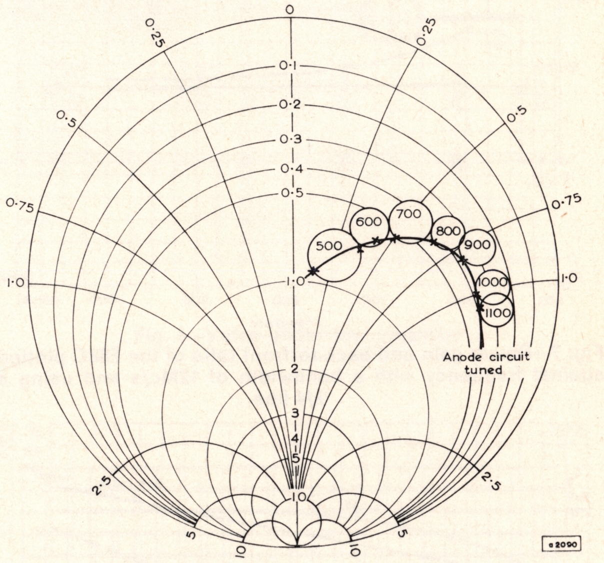

Fig. 13—Variation of input impedance of the E88C with anode tuning at a constant bandwidth of 10Mc/s. The centre frequency for each set of measurements varies in 100Mc/s stages from 500Mc/s to 1100Mc/s

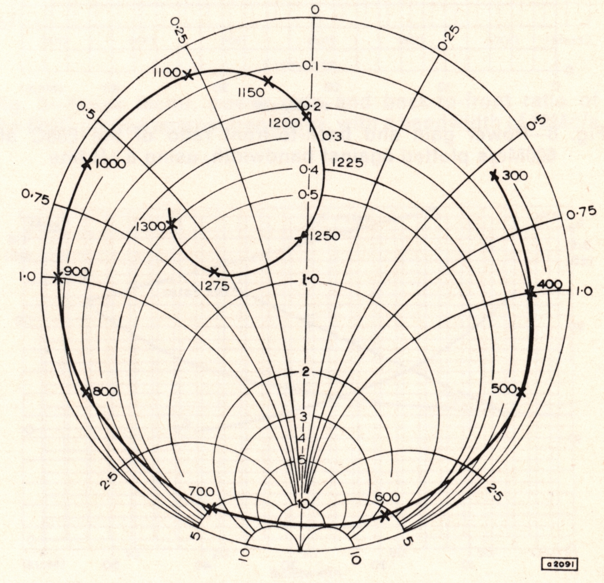

Fig. 14—Variation of cold input admittance with frequency for the E88C (Output short-circuited)

The variation of input impedance with anode circuit tuning is made with the circuit arranged for maximum power gain at the required bandwidth, the impedance measurement being made at the cathode pin of the E88C. The amplifier is set up at the desired bandwidth and the input signal frequency varied while the resulting changes in impedance are plotted on the Smith chart. The results of measurements from 500Mc/s to 1100Mc/s with a bandwidth of 10Mc/s are given in Fig. 13.

Cold Input and Output Admittance

Measurements have been made from 300Mc/s to 1500Mc/s of the cold input and output admittances. The results are shown in Fig. 14 and Fig. 15. In the measurement of input admittance, the diagraph is connected to the cathode of the E88C, the heater leads are 'left floating' or disconnected, and the other electrodes are earthed. In the measurement of output admittance the diagraph is connected to the anode, the other electrodes are earthed, and the heater remains disconnected.

APPLICATIONS

The E88C may be used at frequencies up to and above 1000Mc/s in many single stage applications, and as part of more complex equipment using these frequencies. Three single-valve amplifier stages are described first, followed by four complete receiver front ends.

Several prototype front ends for receivers operating at various frequencies have been constructed. Two of these, for the 470Mc/s band, are described in this article, one using a valve mixer and the other using a crystal diode mixer. Two front ends for the 960Mc/s band are also described; again, one uses a valve mixer and the other a crystal diode mixer.

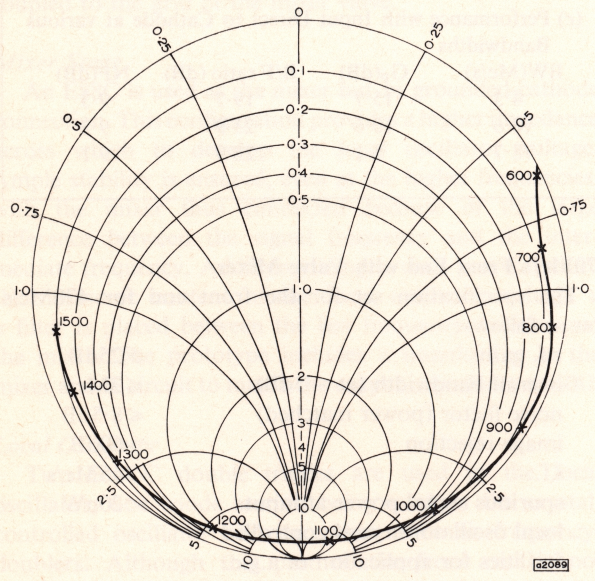

Fig. 15—Variation of cold output admittance with frequency for the E88C (Input short-circuited)

Single Stage λ/2 Trough-line Amplifier

The circuit of a single stage trough-line amplifier using a λ/2 (half wavelength) output line is shown in Fig. 4. This circuit is the one used in the valve-under-test amplifier for measuring valve performance. The frequency range over which the circuit is satisfactory in operation extends to about 1400Mc/s, provided that suitable lengths of anode line are used in the output circuit and suitable inductances used in the input π filter. The purpose of the π filter is to match the generator output impedance to the valve input impedance. The output λ/2 trough-line can be tuned by a variable capacitor connected between the chassis and the end of the line furthest from the valve.

Anode circuit bandwidth is adjusted by varying the coupling between the line and the load. This coupling can be effected by a small ceramic capacitor, which, with its associated lead, can be used to give a combination of inductive and capacitive coupling; such coupling facilitates the adjustment of bandwidth between valve samples.

An alternative form of anode circuit, still with a λ/2 line, has two trimming capacitors attached to the line, one at each end. By adjusting these two capacitors the effective position of electrical connection of the fixed tap can be altered, thus changing the coupling and bandwidth.

The r.f. choke in the cathode lead is necessary to prevent damping of the input circuit by the cathode bias resistor. In addition, r.f. chokes are put in the heater and h.t. supply leads.

A well-soldered screen is recommended for keeping separate the input and output circuits. Internal feedback in the E88C is so low that, even with narrow bandwidths at frequencies in excess of 1000Mc/s, instability is unlikely if the external screening is satisfactory.

Single Stage λ/4 Trough-line Amplifier

The circuit of a typical single stage amplifier using a λ/4 (quarter wave-length) anode line is shown in Fig. 16. This circuit has been made to operate at frequencies up to 1000Mc/s. The λ/4 line has a higher efficiency than the λ/2 line and so greater gains are obtainable with it.

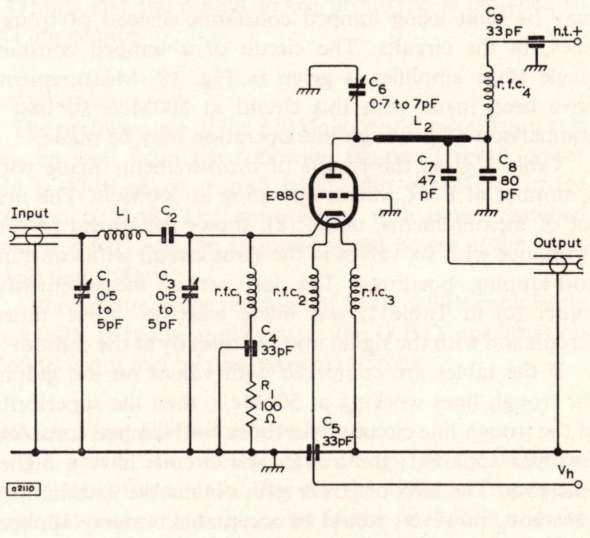

Fig. 16—Single-stage amplifier using λ/4 line

The performance of the λ/4 line amplifier may be compared with that of the λ/2 line amplifier by reference to Figs. 6 to 9. Single valve operation can provide high levels of power gain at u.h.f., but where maximum gain is essential the λ/4 line is superior to the λ/2 line.

The photograph shown in Fig. 17 is of a prototype λ/4 amplifier. This indicates a suitable layout of the components intended to operate at u.h.f., and the degree of shielding necessary. At the higher frequencies the inductance of the input π filter is formed by the leads of the variable capacitor shown at the lower end of the photograph.

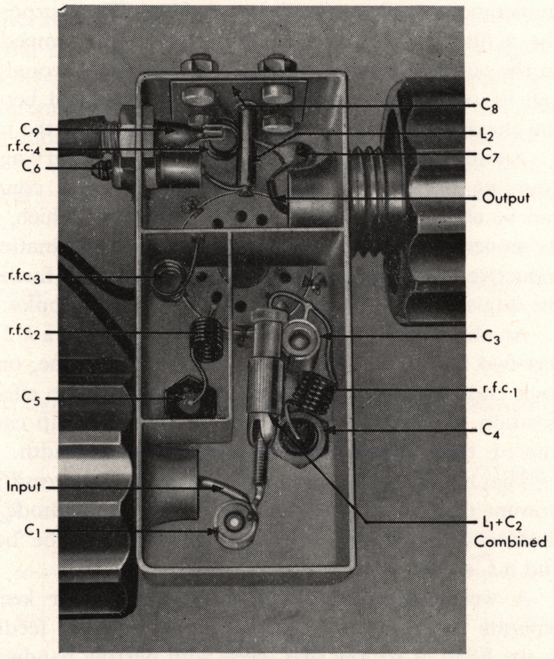

Fig. 17—Layout of the λ/4 amplifier. The inductance of the π filter is formed by the leads to the variable capacitor. The input is at the lower end of the photograph

Single Stage Amplifier with Lumped Circuit Constants

Amplifiers using the E88C and operating at u.h.f. may be built using lumped constants, instead of trough lines, in the circuits. The circuit of a lumped constant single stage amplifier is given in Fig. 18. Measurements have been made with this circuit at 500Mc/s so that a comparison with trough line operation may be made.

Table 1 gives the results of measurements made with a number of E88C valves operating at 500Mc/s. The first set of measurements, under (a), shows the spread in performance with six valves in the same circuit with constant coil-tapping positions. The last set of measurements, under (c) in Table 1, was made with no input tuned circuit and with the signal injected directly at the cathode.

If the tables are compared with values on the graphs for trough lines working at 500Mc/s, then the superiority of the trough line circuits over those with lumped constants becomes apparent; the trough line circuits have a higher efficiency. The level of power gain obtainable with lumped constants, however, would be acceptable in many applications.

The table also indicates that even without a tuned input circuit the performance of the E88C is completely acceptable in most applications.

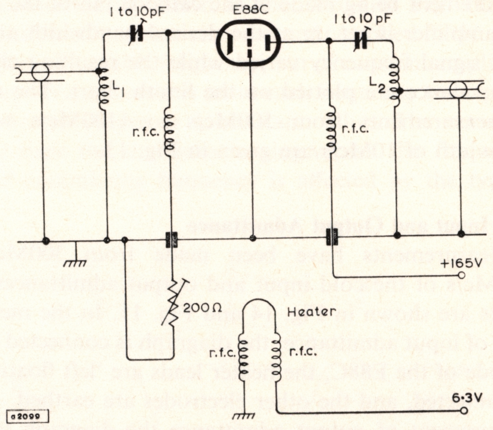

Fig. 18—Single stage amplifier using lumped-constants

TABLE 1

Performance of E88C with Lumped Circuit Constants

BW(Mc/s)	G_p(dB)	B/F ratio (dB)	NF(dB)
(*a*) Performance with Constant Tapping Positions			
9·0	13·2	25·0	7·2
9·0	13·6	23·1	7·6
9·5	13·7	23·1	7·4
10·0	13·4	23·9	7·8
10·0	13·6	24·4	8·1
10·0	13·7	23·3	7·2
(*b*) Performance at various Bandwidths			
BW(Mc/s)	G_p(dB)	B/F ratio (dB)	NF(dB)
3·0	17·8	18·0	7·3
17·5	11·1	24·2	7·0
71·5	6·9	28·5	7·6
(*c*) Performance with Input Direct to Cathode at various Bandwidths			
BW(Mc/s)	G_p(dB)	B/F ratio (dB)	NF(dB)
4·3	15·7	19·7	9·3
18·6	10·6	23·9	9·3
78·7	6·1	28·9	9·1

470Mc/s Front End with Valve Mixer

The specification set for the front end for 470Mc/s was as follows:

r.f. gain	⩾25dB
overall bandwidth (at −3dB)	⩽2Mc/s
noise factor (power matched)	⩽8·5dB
image rejection	>60dB
i.f.	45Mc/s
spurious signal power at input	<20nW
local oscillator crystal controlled	
facilities for application of a.g.c.	

The front end consists of two grounded-grid r.f. stages, the valve mixer and the crystal controlled local oscillator. Two r.f. stages are included in the design to obtain the following advantages:

- the required r.f. selectivity can be obtained without recourse to complicated filters;
- gain control can be applied to the second r.f. stage and so the a.g.c. will have very little effect on the input matching of the first stage to the aerial;
- the valve mixer will contribute only a negligible amount to the overall noise factor;
- oscillator radiation at the aerial is minimised.

The circuit of the complete front end is given in Fig. 19 and details of the circuit and performance are given below.

R.F. Stages

The first grounded-grid E88C has a π filter to match its input to the aerial. A bandpass filter consisting of two λ/4 trough lines forms the anode load. As only a small amount of coupling between the primary and secondary is needed, it is achieved by 'shorting' both to the same earthed screen to which is also connected a small adjustable coupling loop. The filter is tuned with the variable capacitors at the high impedance ends of the lines. The shorting of the primary line is simplified by the d.c. blocking capacitor. To prevent excessive damping of the secondary, the second r.f. stage is coupled only loosely to the filter. The gain of the first stage is high because the bandwidth can be made as low as 3Mc/s.

Automatic gain control is applied to the second r.f. stage. This necessitates using a capacitor to short the grid to earth at the signal frequency. This capacitor, in the prototype, consists of sheets of mica sandwiched between the central earthing shield and two copper sheets to which the grid pins are soldered; the plates are bolted to the centre screen with nylon bolts. The minimum total capacitance of this device is about 200pF

The gain of the second stage is made lower than that of the first stage to prevent excessive changes in input admittance when a.g.c. voltages are applied. The output circuit of the second stage is a λ/2 trough line inductively coupled to the grid of the mixer valve.

Mixer Stage

An E88C is used as the mixer but in grounded-cathode connection. This configuration provides a higher impedance across which to develop the local oscillator voltage. Ample stability is ensured, even at the higher frequencies, with the mixer thus connected because of the large difference between the signal frequency and the intermediate frequency. Additive mixing is used and to reduce the harmonic content of the local oscillator voltage a π filter is placed between the last frequency-doubler and the mixer. The prototype includes a transformer in the mixer anode circuit to match the output impedance to 60Ω.

Local Oscillator

Two E88CC double triodes are used in the local oscillator, one triode section being used as the crystal-controlled oscillator and the other three as frequency-doublers. Although this part of the front end is not considered in this article, details are included in the circuit diagram (Fig. 19).

Performance

The performance of the front end design can be seen from measurements made on one prototype. The overall power gain of the two r.f. stages and mixer is 40dB with an overall bandwidth of 1·9Mc/s. Overall noise factor for the three stages is 8·0dB with a power matched input circuit. The gain is controllable over a range of 30dB with negligible influence on the input impedance. Image rejection varies with applied a.g.c. voltage from a maximum of >85dB to a minimum of 65dB. The measured level of spurious power at the input socket is less than 250pW.

470Mc/s Front End with Crystal Diode Mixer

The specification for the front end with a crystal diode mixer is exactly the same as that for the front end with a valve mixer previously described. The front end consists of one E88C r.f. stage, in grounded-grid connection, followed by the crystal diode mixer and then by an E88CC cascode i.f. amplifier. This high-gain, low-noise amplifier helps to keep the noise figure of the complete front end to a minimum as, although the crystal mixer produces less noise than a valve mixer it has about a 7dB insertion loss. The complete circuit diagram is given in Fig. 20.

R.F. Stage

In the anode circuit of the r.f. stage a λ/4 line bandpass filter is used. The gain of this stage alone is 18dB with a bandwidth of 3Mc/s.

Crystal Mixer, Local Oscillator and I.F. Stage

Frequency changing is accomplished by the crystal mixer which, in the prototype, was type 1N82A. This crystal was connected through a capacitor at a tapping point on the secondary λ/4 line of the bandpass filter. The local oscillator drive should maintain a crystal diode current of 0·5mA, the recommended value for the diode in this application. The drive required from the oscillator to maintain this current is considerably less than that required to operate a valve mixer.

The i.f. amplifier stage is a conventional series cascode circuit using the two parts of an E88CC. The i.f. frequency is 45Mc/s and the output in the prototype is matched to 60Ω impedance.

Performance

The performance of the 470Mc/s crystal mixer front end may be seen from the following figures. Overall power gain is 37dB at an overall bandwidth of 1Mc/s: image rejection is 52dB. The noise factor with power-matched input is 8·5dB and the spurious signal power at the input is less than 100pW.

Although the image rejection of 52dB will be completely acceptable in many applications, the G.P.O. specification of 60dB is not met by this particular circuit.

960Mc/s Front End with Valve Mixer

The specification set for the design of the 960Mc/s front ends is the same as that for the 470Mc/s front ends (page 84) except that the noise factor is 12·5dB and the intermediate frequency is 50Mc/s. The front end consists of two r.f. stages, the crystal controlled local oscillator and valve mixer. Details of the circuit are described below, and the circuit is shown in Fig. 21.

R.F. Stages

Two r.f. stages are used to attain the necessary values of gain and selectivity without the use of complicated filters, and to reduce oscillator radiation through the aerial to an insignificant level. The first r.f. stage has a π filter to match the input impedance of the E88C to the aerial. A bandpass filter consisting of two λ/2 lines with a common inductance forms the anode load of this stage. Coarse coupling control is effected by selecting the value of the common inductance, and fine control by varying the effective tapping position of the second stage in the secondary line. This 'effective tapping position' in the λ/2 line can be varied by adjusting the variable capacitor at each end, thereby varying the position of the standing wave rather than the physical tapping point.

The anode load of the second stage is a λ/2 line, having capacitors at each end for the same purpose as those mentioned above. The output to the mixer stage is taken from the tapping point.

Valve holders in the r.f. stage should preferably be of the wafer-thin type, so that the grid pins can be earthed with the shortest possible leads. All supply wiring in the prototype is kept to the top of the chassis and taken through the chassis with lead-through capacitors: this procedure minimises stray couplings through the inductances and capacitances of parts of the supply lines.

Mixer Stage

The valve mixer consists of a grounded-grid E88C; the five grid pins of the E88C are earthed through five separate capacitors, four through 15pF capacitors to give effective r.f. earthing and one through a 3·3nF capacitor to give effective i.f. earthing.

In the anode circuit of the mixer is a transformer tuned to 50Mc/s. The output impedance was 60Ω from this transformer in the prototype.

Local Oscillator Stage

Five stages are used in the local oscillator; two E88CC double triodes are used to provide the oscillator and first three frequency doubler stages using the half-valves separately, and one E88C is used as the final doubler. Grounded-cathode configuration is used with the two E88CC valves and grounded-grid for the E88C. To reduce the level of spurious harmonics, double tuned coupling circuits are used between the multiplier stages.

Performance

The following figures indicate the performance of the design. The gain of the r.f. stages alone is 30dB at a bandwidth of 2Mc/s, while the overall gain of the front end is 34dB at a bandwidth of 1·5Mc/s. Image rejection is 70dB and the noise factor 12·4dB. Spurious power measured at the input socket is about 10nW.

960Mc/s Front End with Crystal Diode Mixer

Only a few differences exist between the two circuits for 960Mc/s front ends using crystal and valve mixers. Most of these are concerned with only the mixer stage, and details of the mixer stage and overall performance are given below. The circuit is shown in Fig. 22.

Crystal Diode Mixer Stage

The signal and oscillator frequencies are fed to one side of the crystal diode (type 1N82A) and the other end of the diode is connected to a tapping point on the input coil of the i.f. amplifier. The tapping point should be selected to give minimum noise. Oscillator drive is adjusted to give a direct current in the crystal of 0·5mA, the recommended value for this application.

One E88CC double triode is used as the first i.f. amplifier and is connected in series cascode. This amplifier is neutralised to give a low noise figure for the stage. The low noise i.f. amplifier is required because of the 7dB insertion loss of the crystal diode. This 7dB loss has no appreciable effect on the overall noise factor of this front end because of the high gain in the r.f. stages. Should r.f. stages with lower gains be constructed, however, the contribution of the i.f. stages to the overall noise factor should be minimised.

Performance

The gain of the r.f. stages alone is 30dB at a bandwidth of 2Mc/s. Overall gain is 53dB at a bandwidth of 1·3Mc/s. Image rejection is 73dB and noise factor 12·4dB. The spurious power at the input socket is 64pW.

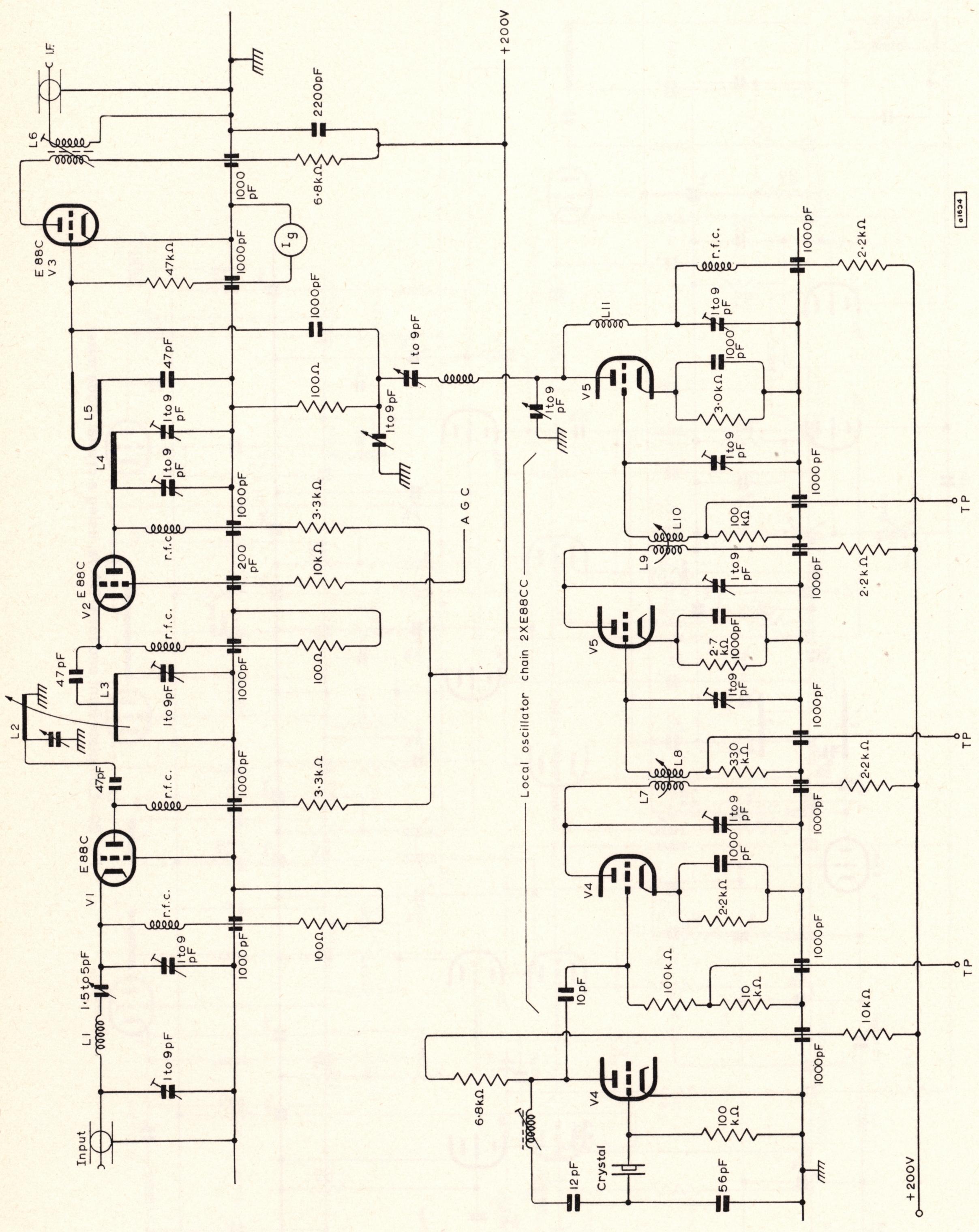

Fig. 19—Complete front end for 470Mc/s, using a valve mixer

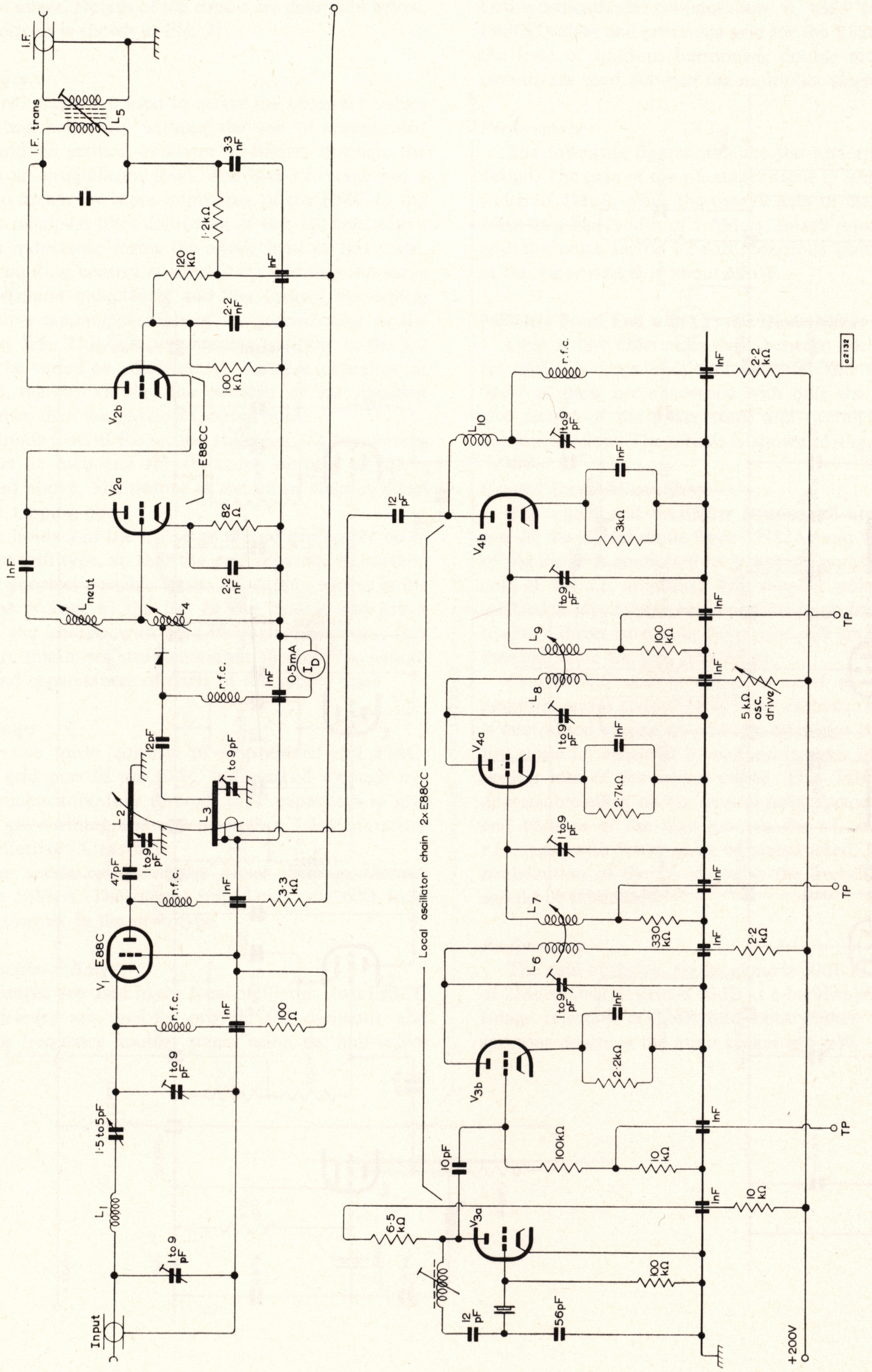
Input
E88C
V_1
L_1
1·5 to 5pF
1 to 9 pF
r.f.c.
47pF
L_2
L_3
1 to 9pF
12pF
1nF
3·3 kΩ
100 Ω
L_4
L_{neut}
0·5mA
I_D
V_{2a}
V_{2b}
E88CC
82 Ω
22 nF
2·2 nF
100 kΩ
120 kΩ
1·2kΩ
33 nF
I.F. trans
L_5
I.F.
Local oscillator chain 2×E88CC
V_{3a}
V_{3b}
V_{4a}
V_{4b}
L_6
L_7
L_8
L_9
L_{10}
12 pF
56pF
10pF
6·5 kΩ
100kΩ
10 kΩ
2·2kΩ
330 Ω
2·7kΩ
3kΩ
5 kΩ osc. drive
TP
+200V
a2132

Fig. 20—Complete front end for 470Mc/s, using a crystal diode mixer

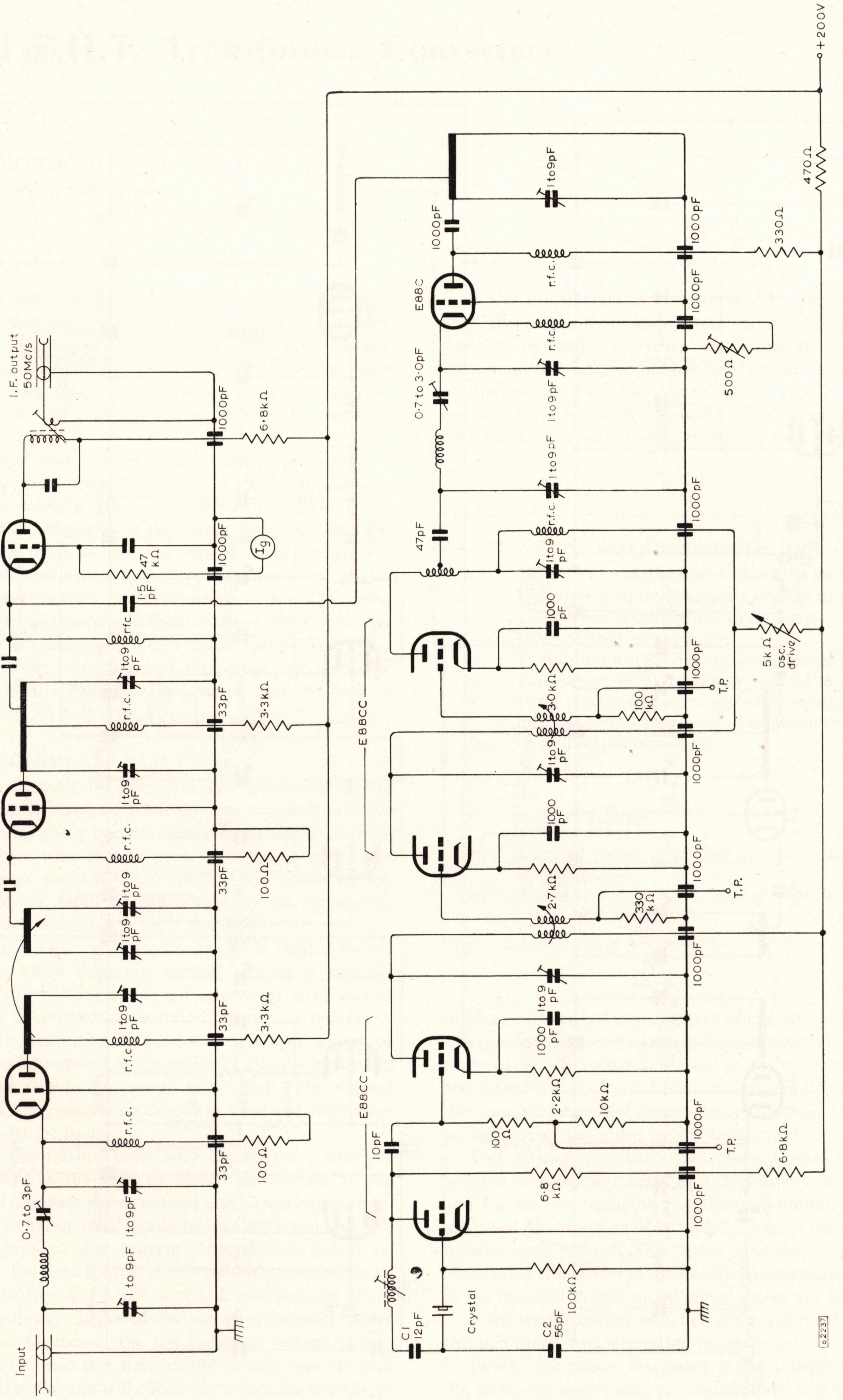
Input
E 88C
I.F. output 50Mc/s
0·7 to 3pF
1 to 9pF
r.f.c.
33pF
3·3kΩ
100 Ω
22pF
4·7pF
1·5 pF
47 kΩ
1000pF
6·8kΩ
Ig
E88CC
C1 12pF
Crystal
C2 56pF
100kΩ
10pF
6·8 kΩ
2·2kΩ
10kΩ
2·7kΩ
330 Ω
T.P.
5kΩ osc. drive
47pF
0·7 to 3·0pF
500 Ω
330 Ω
470 Ω
+200V
a2233

Fig. 21—Complete front end for 960Mc/s using a valve mixer

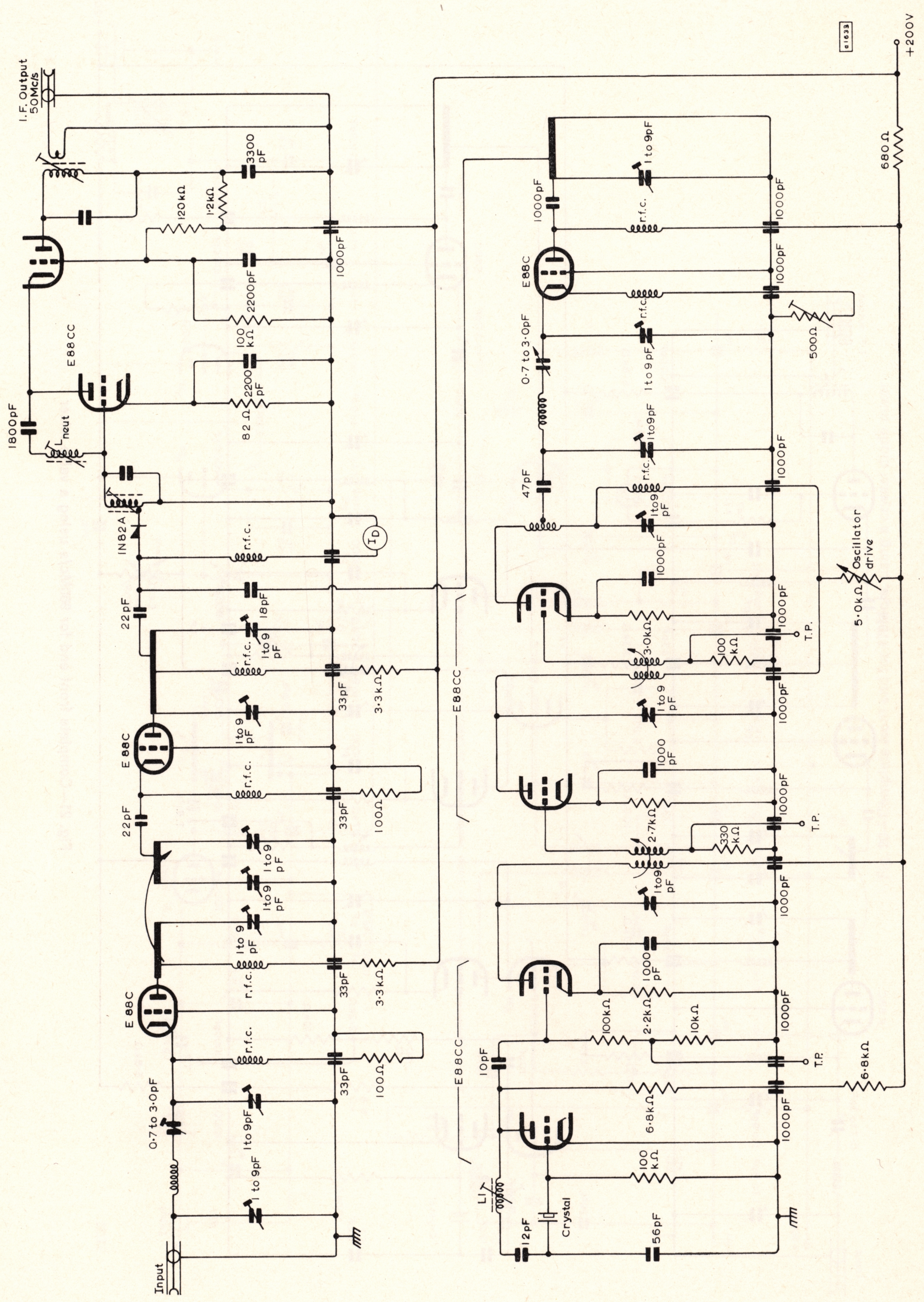

Fig. 22—Complete front end for 960Mc/s using a crystal diode mixer

Tuned E.H.T. Transformer Converters

T. H. BEEFORTH
Mullard Research Laboratories

The design and operation of transistor transformer converters for generating e.h.t. voltages from a low voltage source are considered. It is shown that, by carefully allowing for transformer leakage inductance and stray capacitance, the peak output voltage generated by the transformer is well above that given directly by the turns ratio.

If the total converter losses are assumed to be proportional to the mean square of the current flowing through the transformer primary, then it is shown that there is an inverse relationship between the output impedance and the mean off-load input current; this may be useful to designers who want the minimum values of both parameters.

The article includes practical details of two 12V units, both capable of supplying 100μA at about 16kV. One has low output impedance and high input current (12·5MΩ, 900mA) and the other has high impedance and low input current (35MΩ, 150mA). The overall size of both is approximately $2\frac{3}{4} \times 2\frac{3}{4} \times 5$in.

INTRODUCTION

The e.h.t. supply for television and radar cathode ray tubes is usually obtained from the line scanning circuits. This is possible partly because these circuits already include a transformer with a high peak voltage per turn, and partly because the additional energy requirement of the e.h.t. supply is small in proportion to the circulating energy already available in these circuits.

Sometimes, however, an e.h.t. supply is needed for an application which does not already include a suitable transformer or has not a high enough energy level, and in these cases, a completely separate unit may be necessary. For example, scan magnification was developed to reduce the power consumption of the scanning circuits by having much lower circulating energy than usual. The normal methods of e.h.t. generation cannot be used and alternative means have to be found.

The investigation into tuned e.h.t. transformer converters was instigated by the work on scan magnification. It was clear that a compact self-contained unit capable of supplying 100μA at about 16kV would be necessary and that low output impedance and current consumption would be important. The need for low power consumption and small size, and the fact that a 12V supply is conveniently available, immediately suggested the use of transistors rather than valves. Moreover, the low collector voltage ratings of transistors mean that transformer circuits may be used since a high turns ratio will effectively isolate the transistors from the high voltage side of the converter.

If the transformer is wound so that the turns ratio itself gives the full voltage step-up (of about 1500), it will possibly be rather unwieldy and large. It is therefore advantageous to use further methods for additional voltage multiplication. Two such methods are considered here; one involves the straightforward use of multipliers (incorporating rectifiers, for example) and the other uses the ringing properties of transformers which have considerable leakage inductance and stray capacitance (L_o and C_o respectively, as referred to the primary). Although L_o and C_o are usually looked upon as unavoidable nuisances, they can, under certain circumstances, increase the voltage output above that given by the turns ratio.

LIST OF SYMBOLS

a	Fraction to which output voltage falls on load
C_o	Transformer stray capacitance referred to primary
C_s	Transformer primary shunt capacitance
$I_{in(av)}$	Mean off-load input current
L_o	Transformer leakage inductance referred to primary
L_s	Transformer shunt inductance referred to primary
N	Turns ratio of equivalent perfect transformer
Z	Inherent output impedance of transformer
Z_{out}	Overall output impedance
α	$\frac{R}{2L_o}$
β	$\left[\frac{1}{L_oC_o} - \left(\frac{R}{2L_o}\right)^2\right]^{\frac{1}{2}}$
τ	Resonant period of leakage inductance and stray capacitance
$\omega/2\pi$	Resonant frequency of leakage inductance and stray capacitance

This article investigates the different ways of driving suitable transformers (that is, transformers in which L_o and C_o are not negligible) so that the output voltage is increased by the action of L_o and C_o, and at the same time remains well defined. This latter condition is important when using transistors in the waveform generator and leads to the conclusion that only voltage drives are feasible.

If the transistors are switched while a current is flowing through them, two interesting points arise:

Firstly, the power dissipated in the transistors during the switching time γ may be considerable, and apart from the large current making the switching more difficult, there is the possibility of the peak power damaging the transistors.

Secondly, large transient voltages could be induced in the inductive load on turn-off. Although at first this sounds quite an attractive possibility for deriving a high voltage, in actual fact the peak output voltage would not be well defined because the amplitude of the transients will be very dependent on the time γ, which is the transistor 'turn-off' time. If the transition from 'on' to 'off' is being made as rapidly as possible, the period γ will be determined mainly by individual transistor characteristics and will vary considerably from one transistor to another.

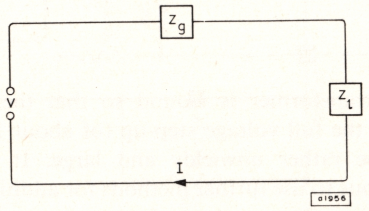

Fig. 1—Generator operating from low impedance voltage supply

For these reasons, the analysis will include only those switching modes in which theoretically no current is flowing immediately before and after a transition. This precludes the use of current sources for the initial d.c. supply.

The generators considered here are intended to operate from a low impedance d.c. supply such as a battery, and may be represented as the variable impedance Z_g shown in Fig. 1. The load impedance is a constant Z_l. Therefore

$$I(t) = \frac{V}{Z_g(t)+Z_l}.$$

If

$$Z_g(t) = R_g(t)+jX_g(t),$$

then the power dissipated in the waveform generator is

$$P(t) = \frac{V^2R_g(t)}{\{R_g(t)+jX_g(t)+Z_l\}^2}.$$

To minimise this power, $R_g(t)$ must always be zero or infinite. In other words, the waveform generator reduces to the connection of the voltage supply to the transformer via a circuit element whose resistance is zero or infinite. The 'perfect switch' chosen here is the transistor, and at all times this will be kept either fully on (bottomed) or cut-off.

When an alloy-junction transistor is bottomed, the collector to emitter resistance has a reasonably constant value which is independent of the collector current that is flowing. Therefore, the transistor losses, which account for a considerable part of the driving circuit losses, may be assumed proportional to the square of the collector current.

Consideration is given to various methods of using transformer leakage inductance and stray capacitance to advantage, subject to the condition of zero-current switching. The basic principle of these methods is that suitable waveforms will produce peak secondary voltages which are in excess of those given by the turns ratio of the transformer.

ANALYSES OF TUNED TRANSFORMER

General Considerations

In almost every use of transformers, the leakage inductance and stray capacitance are either completely neglected or treated as unavoidable degradations of the transformer. Fig. 2 shows the equivalent circuit of a transformer and from this it can be seen that L_o and C_o do in fact form a series circuit, and that the voltage applied to the terminals of a 'perfect transformer' is the voltage across C_o and not the true drive voltage. Hence, it is quite feasible that certain waveforms will give a larger peak voltage across C_o than is present in the input supply.

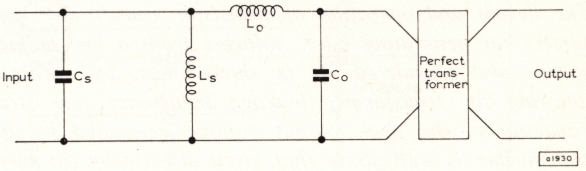

Fig. 2—Equivalent circuit of transformer

For reasons already given, only rectangular voltage drives with zero-current switching are described. This type of drive improves the chances of generating predictable output levels and also simplifies the design of the switching circuits.

When a step voltage is applied to a series L_oC_o circuit, the resulting waveforms of both current and capacitor voltage are as shown in Fig. 3. If there is no further change in the applied voltage, the voltage developed across C_o, that is, V_{Co}, will oscillate about the applied voltage with a peak-to-peak amplitude equal to twice the applied voltage.

There are two different stages in this oscillation at which the current flowing is zero: those times at which V_{Co} equals twice the applied voltage and those times at which V_{Co} is zero. The switching of the drive waveform is practicable at either of these stages.

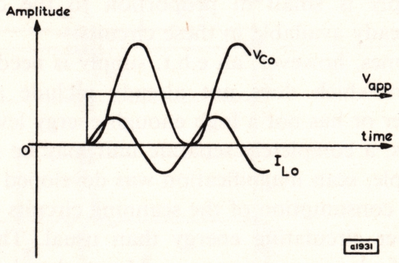

Fig. 3—Waveforms generated on applying step function to series L_oC_o circuit

When V_{Co} equals twice the applied voltage, energy remains in the circuit when the applied voltage is switched back to zero, and when V_{Co} is zero, all the energy supplied to L_o and C_o has been returned to the source. Hence, when the applied voltage is switched in the latter mode, the circuit will remain with zero energy until the applied voltage is again switched to a finite value. This difference in energy level at zero currents is used as the basis for dividing the analyses into two different modes.

The output from the high-energy switching drive is quite different from the output of the low-energy switching drive. The waveform of the high-energy switching drive has a considerable component equal in frequency to the resonant frequency of L_o and C_o and thus resonant amplification occurs; the output voltage is therefore highly dependent on the circuit Q-factor. It is usually difficult to know the value of Q without making measurements, and this makes the design of this mode rather a matter of trial and error. It should only be undertaken if several identical units are to be built. With the low-energy switching drive, however, the peak output will be approximately twice the step voltage times the turns ratio and is almost independent of the circuit Q-factor.

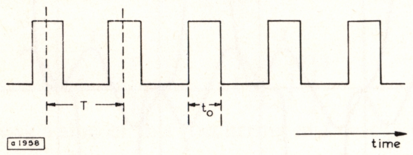

Fig. 4—General rectangular waves form

Both classes of drive waveforms are dealt with, and both single-ended and push-pull drives are applicable. In the analyses it is assumed that the transformer is always shunted by a low impedance in the drive circuitry so that, if a push-pull system is used, one or the other of the transistors must be 'on'.

The voltage-current relationship of the output rectifiers must be taken into account when the impedance of the converters is being calculated. If the exact characteristic curve is used, the calculation becomes excessively involved, and in the analyses it is assumed that the forward resistance is zero and that the reverse resistance is infinite.

As all the drives considered are voltage drives, the effect of the transformer primary shunt inductance (L_S) and primary stray shunt capacitance (C_S) can easily be found if necessary. Their presence will not alter the output characteristics of the converters because of the low impedance of the voltage drives. However, the small additional current flowing through the primary shunt inductance and capacitance will contribute to the overall converter losses.

The currents associated with L_S and C_S are quite separate from those of L_o and C_o and the perfect transformer shown in Fig. 2, and may be neglected if their r.m.s. values are small compared to that of the input current. Normally, this presents no difficulty — for instance, the r.m.s. currents I_{LS} and I_{CS}, of the units described in this article could be neglected by making L_S at least several hundred microhenrys and C_S not more than about 0·1 microfarads. These values can easily be attained.

Switching when Stored Energy is a Maximum

A perfectly general rectangular waveform is shown in Fig. 4. The period of resonance of L_o and C_o is τ, and t_o is less than T. The waveform amplitude is A_o.

First, the relation between t_o, T and τ must be known, so that at the instants of switching, the current flowing through L_o is zero and the voltage developed across C_o is a maximum. If the waveform is split into its Fourier components, then only that with a period equal to τ will deliver an appreciable current through L_o and C_o, and the other harmonics may be neglected at a first approximation. Since L_o,C_o will resonate at this harmonic, the current through L_o and C_o will be in phase with the harmonic voltage and will be zero when this voltage is zero.

The voltage across C_o will be $\pi/2$ out of phase with the current flowing, so that when the current of L_o is zero, maximum energy is stored in C_o. Thus, provided the switching occurs when the current is zero, the energy stored in the resonant circuit will be at the correct high level.

It is shown in Appendix 1 that for switching to occur at zero current, the relationships between T, t_o and τ are:

$$T = n\tau,$$

and

$$t_o = \left(\frac{2p+1}{2n}\right)\tau,$$

where n and p are integers, and $0 \leqslant p < n$.

Under these conditions the transformer output will be a sine wave of period τ, and the peak amplitude will be:

$$2A_oQ\left(\frac{t_o}{T}\right)\frac{\sin(n\pi t_o/T)}{(n\pi t_o/T)}.$$

The optimum values of p and n must be found so that this amplitude is a maximum.

The factor $2A_oQ/\pi$ is determined by circuit considerations, so that the waveform itself, with variable n, t_o and T, can only influence the term $\frac{\sin(n\pi t_o/T)}{n\pi t_o/T}$, and this will have its maximum value when $n = 1$ and $p = 0$. That is, the optimum square waveform is that in which

$$t_o = \frac{\tau}{2} \text{ and } T = \tau.$$

Only this optimum drive is analysed, but the method can be applied to other suitable drive waveforms if the optimum waveform is not being used, as, for example, when a suitable but non-optimum waveform is already present in some other part of the equipment.

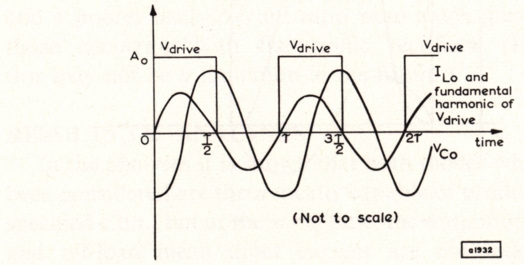

Fig. 5—Waveforms of maximum energy switching off load

Relevant waveforms are shown in Fig. 5. The amplitude of the drive harmonic whose frequency is equal to the resonant frequency of L_o,C_o is:

$$2A_oQ\left(\frac{t_o}{T}\right)\frac{\sin(n\pi t_o/T)}{n\pi t_o/T},$$

and as $n = 1$ and $t_o/T = \frac{1}{2}$, the amplitude is

$$2A_oQ.\tfrac{1}{2}\frac{\sin\pi/2}{\pi/2} = A_o\frac{2}{\pi}Q.$$

Therefore the peak secondary voltage V_{out} is $(NA_oQ)2/\pi$, and is directly proportional to the Q-factor.

The output impedance and off-load input current are often as important as the output voltage level. These are calculated in Appendix 2, the results being that the output impedance Z is given by:

$$Z = 2\pi N^2\left(\frac{L_o}{C_o}\right)^{\frac{1}{2}}$$

where N is the turns ratio, and the mean off-load input current $I_{in(av)}$ is given by:

$$I_{in(av)} = \frac{2A_o}{\pi^2 R}.$$

Since

$$Q = \frac{1}{R}\left(\frac{L_o}{C_o}\right)^{\frac{1}{2}}$$

and

$$V_{out} = \frac{2A_oNQ}{\pi}$$

it follows that there is a relationship between $I_{in(av)}$, Z and V_{out}, dependent only on Q, which is:

$$I_{in(av)}Z = \frac{A_o}{Q}\left(\frac{V_{out}}{A_o}\right)^2.$$

Switching when Stored Energy is a Minimum

When a step voltage is applied to a series L_oC_o circuit, the current and voltage across C_o have waveforms similar to those in Fig. 3. In the absence of any damping, V_{Co} is given by:

$$V_{Co} = A_o(1-\cos\omega t)$$

from $t = 0$, whence

$$I_{Lo} = I_{Co} = C_o\frac{dV_{Co}}{dt} = \omega C_o\sin\omega t.$$

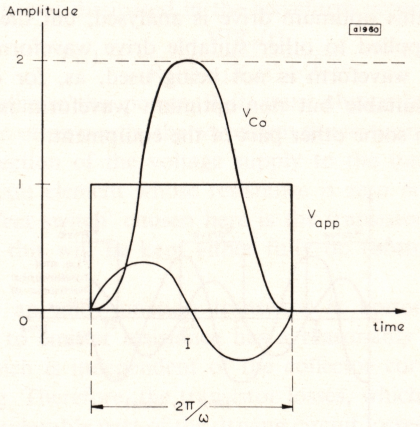

Fig. 6—Waveforms when stored energy is zero

The stored energy is zero when both V_{Co} and the current in L_o, that is I_{Lo}, are zero, and this occurs when $t = 2n\pi/\omega$. The relevant waveforms are as shown in Fig. 6.

The drive waveform may then comprise a series of similar square pulses, each producing an output quite independent of preceding pulses. The lowest output impedance will occur when the rectifier diodes conduct as often and for as long as possible. This implies allowing the interval between pulses to approach zero, but in practice this would introduce further complications and inefficiencies because of residual energy at $t = n\tau$ caused by the finite values of Q. To overcome the difficulty, a push-pull drive, as shown in Fig. 7, may be used and should be the most efficient. This is the waveform that is fully analysed, and results for other waveforms may be found in a similar manner.

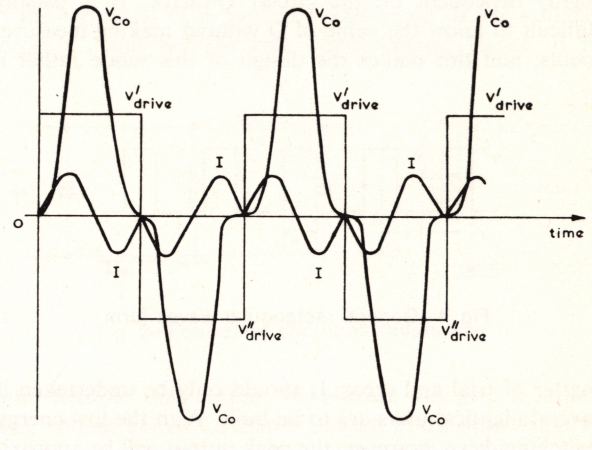

(a) off load

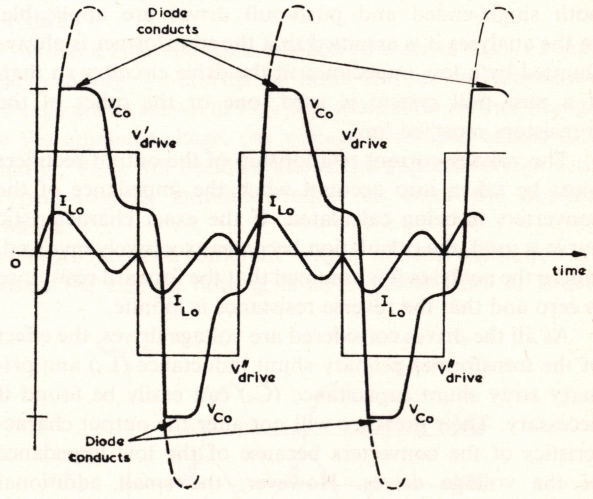

(b) on load

Fig. 7—Waveforms of minimum energy switching

The full analysis of the waveform is given in Appendix 3 and the results of this are:

$$Z = \pi N^2\left(\frac{L_o}{C_o}\right)^{\frac{1}{2}}$$

and

$$I_{in(av)} = \frac{A_oR}{2}.\frac{C_o}{L_o}.$$

Now

$$Q = \frac{1}{R}\left(\frac{L_o}{C_o}\right)^{\frac{1}{2}}$$

and

$$V_{out} = 2NA_o,$$

whence

$$I_{in(av)}Z = \frac{\pi A_o}{8Q}\left(\frac{V_{out}}{A_o}\right)^2.$$

The variation of output voltage with the Q-factor can be found by determining V_{Co} when a step voltage of amplitude A_o is applied to a series L_o,C_o,R circuit. This voltage may be shown to be:

$$V_{Co} = \frac{A_o\{\beta-\exp(-\alpha t)(\beta\cos\beta t+\alpha\sin\beta t)\}}{L_oC_o\beta(\alpha^2+\beta^2)}$$

where

$$\alpha = R/2L_o$$

and

$$\beta = \left[\frac{1}{L_oC_o} - \left(\frac{R}{2L_o}\right)^2\right]^{\frac{1}{2}}$$

and the peak value of this (occurring at $t = \pi/\beta$ when α is small), is given by

$$V_{Co(pk)} = \frac{A_o\beta\{1+\exp(-\alpha t)\}}{L_oC_o\beta(\alpha^2+\beta^2)}.$$

Now, when α is small

$$\alpha^2+\beta^2 \rightarrow \beta^2$$

and

$$\exp(-\alpha t) \rightarrow 1-\alpha t$$
$$= 1 - \frac{R\pi}{2\beta L_o}.$$

Therefore

$$V_{Co(pk)} \rightarrow A_o\left(2 - \frac{1}{2Q}\right)$$

and

$$V_{out} = NA_o\left(2 - \frac{1}{2Q}\right).$$

It can be seen that the variation of output voltage with the Q-factor is much less than in the high energy mode, and as the Q-factor is dependent on the circuit loading, this point weighs heavily in favour of the low energy mode.

Additional Multipliers

As stated earlier, it is possible to increase the voltage from a transformer by a further multiplier. The most common type of multiplier for this purpose is the rectifier multiplier which can give an increase in output voltage of at least two times. It has already been shown that if a transformer is used to give the total voltage step-up, there is then a definite connection between input current and output impedance: how this is affected when a multiplier and transformer with a lower voltage step-up is used is now considered.

If the multiplier is a passive device, that is, no subsidiary energy is supplied to it, and if no energy is dissipated internally, all the energy delivered at the low voltage level must be delivered at the high voltage level. Therefore,

$$E_{in} = E_{out};$$

or

$$V_{in}I_{in} = V_{out}I_{out}.$$

But

$$V_{out} = mV_{in}$$

where m is the multiplication factor. Therefore

$$mI_{out} = I_{in}.$$

Now

$$\Delta V_{out} = m\Delta V_{in},$$

and

$$\Delta I_{out} = \frac{\Delta I_{in}}{m};$$

whence

$$\frac{\Delta V_{out}}{\Delta I_{out}} = \frac{m^2\Delta V_{in}}{\Delta I_{in}}$$

or,

$$Z_{out} = m^2Z.$$

If a total voltage step-up of X is needed, and the transformer gives a voltage step-up of NB, then a multiplier of X/NB must be used.

Even with the use of the multiplier, the relationship between the off-load mean input current and the output impedance is unchanged for either mode. This may be shown in the following way:

$$I_{in(av)}Z = k\left(\frac{V_{out}}{A_o}\right)^2$$

for the two modes considered where Z is the transformer output impedance, V_{out} is the peak transformer output voltage and k is an independent factor of proportionality. Also

$$Z_{out} = m^2Z = \left(\frac{X}{NB}\right)^2 Z.$$

Therefore

$$I_{in(av)}Z_{out} = I_{in(av)}\left(\frac{X}{NB}\right)^2 Z = k\left(\frac{V_{out}}{A_o}\right)^2\left(\frac{X}{NB}\right)^2.$$

But

$$V_{out} = A_oNB$$

so that again

$$I_{in(av)}Z_{out} = kX^2.$$

Theoretically the input power is unaffected by adding multipliers but, in practice, heater power has usually to be supplied, and additional losses are introduced merely on account of the extra components.

If very low input current is needed then low heater power rectifiers will be used which will mean a higher resistance diode and hence higher output impedance. Diodes can be obtained with heater powers of less than 40mW, which is equivalent to about 4mA at 12V.

Non-thermionic diodes were found unsuitable for e.h.t. multipliers because the losses resulting from capacitance and a poorer back-to-front ratio were much greater than those occurring with thermionic rectifiers. (However, this may not be a limitation in the future.)

RESULTS OF ANALYSES

In the analyses it is shown that both modes which have been considered are theoretically capable of producing any specified e.h.t., but at the same time, the output impedance and off-load mean input current are not independent variables. The relationship between off-load mean input current and output impedance is of the form:

$$I_{in(av)}Z_{out} = kX^2.$$

In this equation, X is the total voltage step-up and k is a factor dependent on the mode used and the supply voltage available. The second-power dependence on X illustrates the high input currents or very high output impedances that will be encountered in e.h.t. generators of this kind.

If the mode chosen uses a drive waveform which has a strong harmonic at the resonant frequency of L_o and C_o, then resonant amplification occurs and a high output voltage will be generated. The peak output voltage will be very dependent on Q and this may be a disadvantage for some purposes.

When the drive waveform comprises a series of rectangular pulses, each equal to the resonant period of L_o and C_o, then the output voltage is about twice that which would be given by the turns ratio only. Although this may be lower than in the previous mode, the output level is not so dependent on Q and this means that more predictable outputs can be obtained.

Choice of Mode

There are two factors which decide in favour of the low energy mode for operating tuned transformers.

Firstly, for both the modes considered, a relationship of the form:

$$I_{in(av)}Z_{out} = kX^2$$

has been derived.

However, in the high energy case k is A_o/Q, whereas in the low energy case k is $\pi/8Q$. Hence lower simultaneous values of $I_{in(av)}$ and Z_{out} may be obtained when the low energy mode is used.

Secondly, the output voltage of the high energy mode is directly proportional to the Q-factor in the circuit. As this may not be known in advance, it is difficult to forecast what output will be obtained from a prototype unit. This difficulty does not occur in the low energy mode, where the output voltage is relatively independent of the circuit Q-factor.

Design for high energy operation involves the deliberate introduction of losses into the system so that the Q-factor may be adjusted to give the correct output voltage. This cannot be as satisfactory as the design for low energy operation where the losses are made as small as possible so that the highest Q-factor may be achieved.

For these reasons the sample models were both built to operate in the low energy mode. One was built with a high Q-factor and the other with a lower Q-factor. These give some idea of the range in values for $I_{in(av)}$ and Z_{out} that may be met in converters operating between 12V input and 16 to 18kV output.

PERFORMANCE OF SAMPLE TRANSFORMERS

Two experimental models were made, one having a low output impedance and one having a low power consumption. Square-wave voltage drives were used, the p.r.f. being one-half of the resonant frequency of the leakage inductance and stray capacitance. Ferroxcube cores, type FX2252 were used for both models.

The mean input currents given below were the currents actually supplied to the transformer itself. They do not include the currents in the driving circuit except for those in the collector circuits of the output stage. Because a self-driving circuit with two transistors having a high current gain factor is used, the total mean input current only slightly exceeds the mean current through the transformer primary, and it is this latter current which is of significance when calculating the theoretical output impedance.

Push-pull rectifier multipliers as shown in Fig. 8 were used. These gave a peak voltage step-up of 2½ times, and allowed the use of balanced twin secondaries with low self-capacitance. The twin secondaries may be balanced with respect to earth by winding them in opposite directions. This method of winding also means that the peak secondary voltages occur between the outer ends of the two windings and so minimises the possibility of breakdown between the windings and the core.

All primaries were designed for push-pull drive, the two identical windings being made bifilar. The wire gauge was chosen so that the total primary windings occupied one full-width layer.

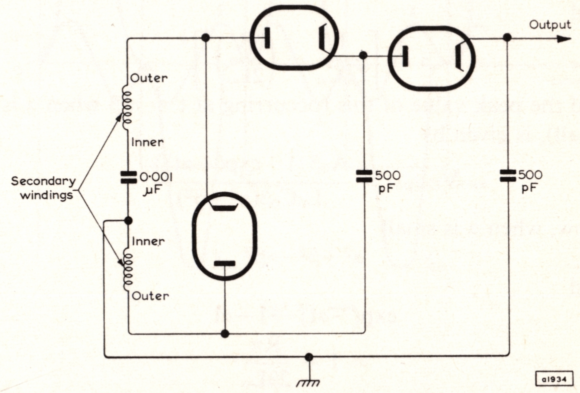

Fig. 8—Rectifier multipler for e.h.t. generator

Low-impedance 16kV Generator

A low impedance, 16kV transformer needs a small L_o/C_o ratio. The leakage inductance is made low by having a small primary inductance (obtained by using only three turns per volt) and winding the secondary on top of the primary. The secondary winding must be made as compact as possible for tightest coupling and so the thinnest wire available should be used. The stray capacitance is increased by using many secondary turns per layer and impregnating the winding with a suitable wax.

As the output impedance is of prime importance, rectifiers with low resistance are chosen for the multiplier. The EY51 valve is selected because it also offers a small size and convenient mounting. Three rectifiers are used and the total heater power consumed is about 1·7W: with good conversion efficiency in the transformer, the input current necessary to heat the rectifiers is about 150mA at 12V. This current is not, of course, related to the output impedance by the rule already stated ($I_{in(av)}Z^2_{out}$) and has to be subtracted from the observed mean input current if the value of $I_{in(av)}Z_{out}/(NB)^2$ is to be calculated.

With the low impedance generator, the total mean input current was 900mA from a 12V supply. The output impedance was 12·5MΩ and the off-load output voltage was 15·5kV. The operating frequency was about 10kc/s. The mean input current was 900–150 or 750mA and the value of $I_{in(av)}Z_{out}/X^2$ was 5·5. This value may be a little higher than necessary since the large circulating current made it difficult to obtain a precise square-wave drive.

The unit can be made as small as $2\frac{3}{4} \times 2\frac{3}{4} \times 4\frac{3}{4}$ in, and may be resin encapsulated if necessary.

Low Consumption 18kV Generator

A low consumption, 18kV transformer needs a high L_o/C_o ratio. The leakage inductance can be made large by using as many as six turns per volt and winding the secondary on a different limb from the primary. Both these measures serve to increase L_o.

The stray capacitance can be kept small by wave-winding the two secondaries with a very open weave. The wire used can be 46 s.w.g. enamel s.s.c. with each secondary of 9600 turns being 0·2in long and 0·75in high.

Rectifiers having very low heater powers, were used, and the total power of three of these rectifiers is just over 0·1W. This is equivalent to an input current of about 10mA at 12V. The mean input current is 150mA at 12V, the output impedance is about 35MΩ and the output voltage is about 18·25kV with the operating frequency about 25kc/s. These figures give a value of:

$$I_{in(av)}Z_{out}/X^2 = 2{\cdot}5.$$

A diagram of the full drive circuit is given in Fig. 9 The unit can be made as small as $2\frac{3}{4} \times 2\frac{3}{4} \times 5\frac{1}{2}$ in.

Comments

These two models probably represent examples of both high and low Q-factor design, and the difference in values of $I_{in(av)}Z_{out}/X^2$ will be mainly due to this. Even with careful design it is unlikely that $I_{in(av)}Z_{out}/X^2$ will ever be less than unity, and this implies a high impedance generator (high Q). Even with careful high Q-factor design, an 18kV generator running from 12V designed to have an output impedance of 10MΩ would need an input current of well over 2A, corresponding to a power consumption of at least 24W.

The two units were built only to show the feasibility of the methods employed, and there is no guarantee of adherence to the component ratings.

CONCLUSIONS

Two main conclusions can be drawn from this article. One relates to the theoretical aspects of utilising transformer leakage inductance and stray capacitance to increase a transformer secondary voltage, and the second relates to the practical possibility of these methods.

The first conclusion is that transformers operating in different modes are subject to restrictions on the mean input current and the output impedance. These two are not independently variable but are linked by an equation of the form:

$$I_{in(av)}Z_{out} = kX^2,$$

where X is the overall voltage step-up and k is a constant dependent only on the particular mode being considered and the input voltage. Further work may show the generality or otherwise of this relationship.

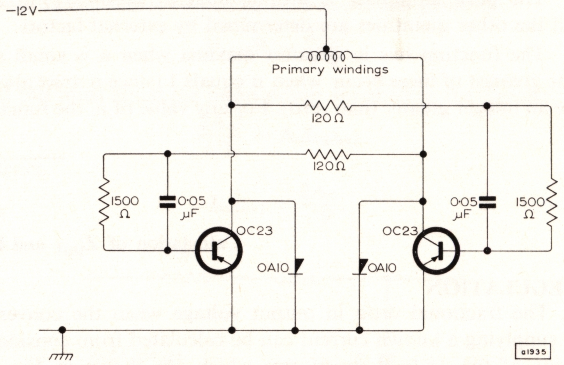

Fig. 9—Drive circuit for low consumption generator

The second conclusion is that these types of tuned transformers are best suited to the generation of high voltages where small size and moderately light weight are important criteria. The large values of k found as yet make it unlikely that these types of tuned transformers will be used for high voltage generation unless very large values of either mean input current or output impedance can be tolerated.

APPENDIX 1

Determination of Optimum Drive Waveform for Maximum Energy Switching

A general rectangular waveform is shown in Fig. 4 (the resonant period of C_o and L_o). The relationship between t_o, T and τ must be determined, so that the current flowing through L_o is zero at the instants of switching. If the waveform is split into its Fourier components only that with a period equal to τ will deliver an appreciable current through L_o and C_o, and the other harmonics may be neglected at a first approximation. Since L_o, C_o will resonate at this harmonic, the current delivered by the source will be almost in phase with the voltage and will therefore be zero when the harmonic voltage is zero.

The amplitude (A_n) of the nth harmonic of such a square wave at time t is given by:

$$A_n = \frac{2A_o t_o}{T} \cdot \frac{\sin(n\pi t_o/T)}{n\pi t_o/T} \cdot \cos\frac{2n\pi t}{T}$$

where A_o is the height of the square, and during any one period this will be zero when t is given by

$$\frac{2n\pi t}{T} = (2p+1)\frac{\pi}{2},$$

where $0 \leqslant p \leqslant (2n-1)$.

At these times, t must equal $+t_o/2$ or $T-(t_o/2)$. Therefore

$$\frac{2n\pi}{T} \cdot \frac{t_o}{2} = (2p+1)\frac{\pi}{2},$$

or

$$T = \frac{2n}{2p+1} t_o,$$

and as $t_o < T$, p may only have values in the ranges $0 \leqslant p < n$. Since L_o and C_o are resonating to the nth harmonic, T must equal $n\tau$, and the relationships between t_o, T and τ are

$$\text{(i) } T = n\tau, \text{ and (ii) } t_o = \left(\frac{2p+1}{2n}\right)\tau,$$

where n, p are integers and $0 \leqslant p < n$.

Under all these conditions, the output of the transformer shown in Fig. 2 will be a sine wave of period τ and the peak amplitude will be:

$$2A_oQ\frac{t_o}{T}\cdot\frac{\sin(n\pi t_o/T)}{n\pi t_o/T}$$

where Q refers to the L_o, C_o circuit.

The upper limit of this function must now be found subject to the above two relationships.

The peak amplitude is proportional to $\sin(n\pi t_o/T)/n$; and all the other quantities are determined by external factors.

The function has its greatest maxima when n is small and the greatest of these occur when n equals 1 (since n must always be an integer greater than zero). For any value of n, the function $\sin(n\pi t_o/T)$ has maximum values when:

$$\frac{nt_o}{T}.\pi = (2q+1)\frac{\pi}{2}$$

that is

$$\frac{t_o}{T} = \frac{(2q+1)}{2n}$$

and this is automatically satisfied when condition (ii) is fulfilled. The optimum waveform is that in which

$$t_o = \frac{\tau}{2}\text{, and } T = \tau\text{, } (n = 1).$$

Other suitable waveforms that could be used are those in which:

$$t_o = \frac{(2p+1)\tau}{2n},$$

and

$$T = n\tau, (n>1,\ 0\leqslant p<n).$$

APPENDIX 2

Calculation of Z_{out} and $I_{in(av)}$ for Maximum Energy Switching

REGULATION

The fractional drop in output voltage when the converter is supplying a known current can be calculated from considerations of the on-load waveforms which are shown in Fig. 10 (half-wave rectification is shown for simplicity).

The load is resistive and is such that V_R has fallen from the off-load value of $(2/\pi)NA_oQ$ to $a(2/\pi)NA_oQ$.

When the diode is not conducting, the voltage across C_o will be a sine wave of amplitude $(2/\pi)NA_oQ$ and lagging behind the relevant input harmonic by $\pi/2$.

When $t = 0$, V_{Co} will rise sinusoidally from E up to F, tending towards G. However, when V_{Co} equals $Na(2/\pi)A_oQ$ the diode will conduct and V_{Co} is now held steady. The current through L_o has been oscillating from A to B, but as the diode conducts, I_{Lo} must fall linearly because:

$$V_{Lo} = Na\frac{2}{\pi}A_oQ - N\frac{2}{\pi}A_o\sin\omega t$$

$$= N\frac{2}{\pi}A_o(aQ-\sin\omega t)$$

and as $aQ \gg \sin\omega t$, V_{Lo} is approximately constant. Therefore

$$\frac{dI_{Lo}}{dt} = -\frac{V_{Co}}{L_o}.$$

The current I_{Lo} now falls to zero linearly at C rather than sinusoidally at D, and this indicates a frequency reduction as a load is applied.

When the diode current (I_d) has fallen to zero, the diode is cut off and leaves L_o and C_o to continue ringing, although initially with reduced amplitude and energy (energy has been supplied to the load, part of which comes from that stored in L_o and C_o). This amplitude builds up and regains its initial value before the diode conducts during the next cycle.

When the diode is conducting, V_{Co} is held fixed (high Q-factor) until I_{Lo} is zero; hence there can be no current flow through C_o. The linear portion of the current waveform must be flowing through the diode into the load, and the diode waveform will be a series of approximately triangular pulses.

For any output voltage it is possible to calculate the current flowing through the diode, and this will give the mean load current. As the fall in output voltage associated with this current is known, the output impedance may be found.

The output voltage is given by:

$$V_{out} = N(2/\pi)aA_oQ\text{ ,}$$

a being slightly less than unity. Then

$$V_{Co} = (2/\pi)A_oQ\sin\omega(t-\tau/4).$$

Now the diode conducts when

$$QaN(2/\pi)A_o = N(2/\pi)A_oQ\sin\omega(t-\tau/4)\text{ ,}$$

or

$$\sin\omega(t-\tau/4) = a\text{ .}$$

At this moment, the value of primary current I_{Lo} (given by C_odV_{Co}/dt) is $\omega C_oA_o(2/\pi)Q\cos\omega(t-\tau/4)$. This current now falls linearly at the rate:

$$\frac{dI}{dt} = -\frac{2aA_oQ/\pi}{L_o},$$

and so the output diode current starts at the value

$$I_{do} = (\omega C_oA_o/N)(2/\pi)Q\cos\omega(t-\tau/4)\text{ ,}$$

and falls at the rate

$$\frac{dI_d}{dt} = -\frac{2aA_oQ}{N_{Lo}\pi},$$

and so flows for a time during each period equal to

$$\frac{2\omega C_oA_oQ}{N\pi}\cos\omega(t-\tau/4)\frac{N_{Lo}\pi}{2aA_oQ}\text{ ;}$$

that is,

$$\frac{\omega C_oL_o}{a}\cos\omega(t-\tau/4).$$

The charge q passed to the load each cycle ($\int idt$) is:

$$q = \tfrac{1}{2}\frac{2\omega C_oA_oQ}{N\pi}\,\frac{\omega C_oL_o}{a}\cos^2\omega(t-\tau/4)\text{ ,}$$

or

$$q = \frac{\omega^2C_o{}^2L_oA_oQ\cos^2\omega(t-\tau/4)}{2N\pi a}.$$

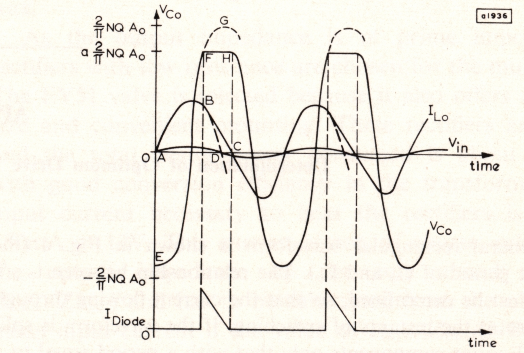

Fig. 10—Waveforms of maximum energy switching on load

With very light loads, a is approximately 1 and the period is almost unchanged. If the period is unaffected, then the mean load current is twice $q\omega/2\pi$ when full wave rectification is used.

Therefore

$$I_{out(av)} = \frac{\omega^3C_o{}^2L_oA_oQ\cos^2\omega(t-\tau/4)}{2\pi^2Na}.$$

Now

$$\sin\omega(t-\tau/4) = a\text{ ,}$$

so that

$$\cos^2\omega(t-\tau/4) = 1-a^2.$$

Therefore

$$I_{out(av)} = \frac{\omega^3C_o{}^2L_oA_oQ(1-a^2)}{2\pi^2Na}\text{ ,}$$

and as

$$\Delta V_{out} = (1-a)NQ(2/\pi)A_o\text{ ,}$$

$$Z = \frac{\Delta V_{out}}{I_{out}}$$

$$= \frac{(1-a)NQ2A_o}{\pi}\cdot\frac{4\pi^2Na}{\omega^3C_o{}^2L_oA_oQ(1-a^2)}.$$

This simplifies to

$$Z = \frac{4\pi N^2a}{\omega^3L_oC_o{}^2(1+a)}\text{ ,}$$

and as

$$\omega^2L_oC_o = 1\text{ ,}$$

and

$$a \simeq 1\text{ ,}$$

then

$$Z = 2\pi.N^2\left(\frac{L_o}{C_o}\right)^{\frac{1}{2}}.$$

Off-load Current Consumption

When there is no output load, the converter will still be dissipating energy because of natural losses which have to be replaced from the input supply. Under certain circumstances these may be considered proportional to the mean square value of the current flowing in the primary and all losses can be lumped as being produced in a frequency independent resistor in series with L_o and C_o (see Fig. 11). At resonance, the current is given by:

$$I = \frac{(2/\pi)A_o\sin\omega t}{j\omega L_o+R+(1/j\omega C_o)}\text{ ,}$$

and the mean square by

$$I^2{}_{(av)} = \frac{2A_o{}^2}{\pi^2R^2}.$$

Hence circuit losses (which equal $I^2{}_{(av)}R$) are given by:

$$I^2{}_{(av)}R = \frac{2A_o{}^2}{\pi^2R}$$

and this must equal the mean power supplied to the circuit;

$$\frac{2A_o{}^2}{\pi^2R} = A_oI_{in(av)}$$

whence

$$I_{in(av)} = \frac{2A_o}{\pi^2R}.$$

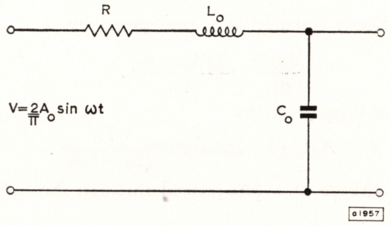

Fig. 11—Off load equivaient circuit

APPENDIX 3

Calculation of Z_{out} and $I_{in(av)}$ for Zero Energy Switching

Where V changes from zero to $+A_o$, a single step voltage starts the output voltage oscillating about the mean level A_o. Natural damping will gradually reduce the amplitude so that no successive peak is as high as the first. If the output load is very light, the diode will only conduct on the first peak, and the passage of enough charge to supply the load current until the next diode conduction period will lead in practice to excessively high voltage-drops across the rectifier. This will subsequently lead to poor regulation.

The most efficient drive waveforms will be those where the output diode or diodes conduct on every high voltage peak generated. The drive waveform should not then have pulses longer than τ before switching to another level. Since the off-load operation during any one period is independent of previous excursions of the voltage, it is justifiable to analyse the off-load circuit behaviour on the application of one square pulse, of length τ, and to modify this analysis suitably to take into account the repetition rate.

Current Consumption

When a step voltage waveform, rising infinitely fast from zero to A_o, is applied to a series circuit of L_o, C_o and R, it may be shown by Laplace transform methods that the current I is given by:

$$I = \frac{A_o}{L_o\beta}\exp\left(\frac{-\alpha t}{2}\right)\sin\beta t$$

where

$$\alpha = \frac{R}{2L_o}$$

and

$$\beta = \left[\frac{1}{L_oC_o} - \left(\frac{R}{2L_o}\right)^2\right]^{\frac{1}{2}}.$$

Therefore

$$I^2 = \frac{A_o{}^2}{L_o{}^2\beta^2}\exp(-\alpha t)\sin^2\beta t\text{ ,}$$

and so the mean square current per pulse is given by:

$$I^2{}_{av} = \frac{\beta}{2\pi}\int_o^{2\pi/\beta} I^2dt.$$

That is

$$I^2{}_{av} = \frac{A_o{}^2\beta}{L_o{}^2\pi\alpha(4\beta^2+\alpha^2)}\left\{1-\exp\left(\frac{-2\pi\alpha}{\beta}\right)\right\}$$

and if R is small, then α will be very much less than β and

$$I^2{}_{av} = \frac{A_o{}^2C_o}{2L_o}.$$

Power dissipated in the circuit must equal power supplied from the voltage source. Therefore:

$$I^2{}_{av}R = A_oI_{in(av)}$$

and

$$I_{in(av)} = \frac{A_oC_oR}{2L_o}.$$

(This will be subject to modification if A_o is zero during any part of a complete cycle of operation.)

Output Impedance

The output impedance depends on the precise form of the drive waveforms. It will be calculated for a case where A_o is not zero for any appreciable time during each period, that is, a push-pull drive will be used. This provides the most effective method of operation.

The analysis is quite general and may be applied to other modes without difficulty.

The on-load waveforms are shown in Fig. 7. When $t = \tau$, it can be seen that the energy in L_o and C_o will not be zero, but because of the diode conduction, not all of the energy stored in the circuit is returned to the supply. The amplitude of oscillation of V_{Co} is thus larger than A_o, and from Fig. 7, the amplitude of the voltage across C_o from $t = n\tau$ until the next time the diode conducts is seen to be:

$$V_{Co} = A_o\{1-(3-2a)\cos\omega t\},$$

where the output voltage level is $(2A_o)a$. Therefore

$$\begin{aligned} I_{Co} &= \frac{C_o dV_{Co}}{dt} \\ &= A_oC_o(3-2a)\omega\sin\omega t. \end{aligned}$$

When $V_{Co} = 2A_oa$, the output diode starts to conduct; that is when

$$2A_oa = A_o\{1-(3-2a)\cos\omega t\},$$

or

$$\cos\omega t = \frac{1-2a}{3-2a}.$$

I_{Co} will then decay linearly at a rate given by

$$\frac{di_{Co}}{dt} = \frac{2aA_o - A_o}{L_o},$$

and so takes a time given by

$$t = A_oC_o(3-2a)\omega\sin\omega t\frac{L_o}{(2a-1)A_o}.$$

Hence the charge $q(= \frac{1}{2}it)$ passed through the output diode is:

$$q = \tfrac{1}{2}L_oC_o\frac{(3-2a)}{(2a-1)}\omega\sin\omega t.\frac{A_oC_o(3-2a)\omega\sin\omega t}{N},$$

which reduces to

$$q = A_oL_oC_o^2\frac{\omega^2(3-2a)^2}{2N(2a-1)^2}\sin^2\omega t.$$

The mean output current $I_{out(av)}$ is given by:

$$I_{out(av)} = \omega q/2\pi.$$

Therefore

$$I_{out(av)} = \frac{A_oL_oC_o^2\omega^3(3-2a)^2\sin^2\omega t}{4\pi(2a-1)^2N}.$$

Now

$$\cos\omega t = \frac{1-2a}{3-2a}.$$

Therefore

$$\sin^2\omega t = \frac{8(1-a)}{(3-2a)^2},$$

so that

$$\begin{aligned} I_{out(av)} &= \frac{A_o\omega C_o(3-2a)^2}{4\pi(2a-1)^2}\cdot\frac{8(1-a)}{(3-2a)^2} \\ &= \frac{2A_o}{\pi N}\frac{(1-a)}{(2a-1)^2}\left(\frac{C_o}{L_o}\right)^{\frac{1}{2}} \end{aligned}$$

and as

$$\Delta V_{out} = (2A_oN - 2A_oNa),$$

then

$$Z = \frac{2A_oN(1-a)}{2A_o(1-a)}.\pi N(2a-1)^2\left(\frac{L_o}{C_o}\right)^{\frac{1}{2}},$$

and as $a \simeq 1$,

$$Z = \pi.N^2\left(\frac{L_o}{C_o}\right)^{\frac{1}{2}}.$$
